INTERIOR PENALTY METHOD FOR THE INDEFINITE TIME-HARMONIC MAXWELL EQUATIONS

PAUL HOUSTON *, ILARIA PERUGIA †, ANNA SCHNEEBELI ‡, AND DOMINIK SCHÖTZAU §

Abstract. In this paper, we introduce and analyze the interior penalty discontinuous Galerkin method for the numerical discretization of the *indefinite* time-harmonic Maxwell equations in high-frequency regime. Based on suitable duality arguments, we derive a-priori error bounds in the energy norm and the L^2-norm. In particular, the error in the energy norm is shown to converge with the optimal order $\mathcal{O}(h^{\min\{s,\ell\}})$ with respect to the mesh size h, the polynomial degree ℓ, and the regularity exponent s of the analytical solution. Under additional regularity assumptions, the L^2-error is shown to converge with the optimal order $\mathcal{O}(h^{\ell+1})$. The theoretical results are confirmed in a series of numerical experiments.

Key words. Discontinuous Galerkin methods, a-priori error analysis, indefinite time-harmonic Maxwell equations.

AMS subject classifications. 65N30

1. Introduction. In this paper, we present and analyze the interior penalty discontinuous Galerkin (DG) finite element method for the numerical discretization of the *indefinite* time-harmonic Maxwell equations in a lossless medium with a perfectly conducting boundary: find the (scaled) electric field $\mathbf{u} = \mathbf{u}(\mathbf{x})$ that satisfies

$$\begin{aligned} \nabla \times \nabla \times \mathbf{u} - k^2\mathbf{u} &= \mathbf{j} \qquad \text{in } \Omega, \\ \mathbf{n} \times \mathbf{u} &= \mathbf{0} \qquad \text{on } \Gamma. \end{aligned} \tag{1.1}$$

Here, Ω is an open bounded Lipschitz polyhedron in $\mathbb{R}^3$ with boundary $\Gamma = \partial\Omega$ and outward normal unit vector $\mathbf{n}$. For simplicity, we assume Ω to be simply-connected and Γ to be connected. The right-hand side $\mathbf{j}$ is a given external source field in $L^2(\Omega)^3$ and $k > 0$ is the wave number, i.e., $k = \omega\sqrt{\varepsilon_0\mu_0}$, where $\omega > 0$ is a given temporal frequency, and ε_0 and μ_0 are the electric permittivity and the magnetic permeability, respectively, of the free space. We point out that we have assumed here that the relative material properties ε_r and μ_r are equal to 1.

By introducing the Sobolev space

$$H_0(\text{curl};\Omega) := \{\, \mathbf{v} \in L^2(\Omega)^3 : \nabla \times \mathbf{v} \in L^2(\Omega)^3,\ \mathbf{n} \times \mathbf{v} = \mathbf{0} \text{ on } \Gamma \,\},$$

the weak form of the equations (1.1) reads: find $\mathbf{u} \in H_0(\text{curl};\Omega)$ such that

$$a(\mathbf{u},\mathbf{v}) := \int_\Omega \left[\nabla \times \mathbf{u} \cdot \nabla \times \mathbf{v} - k^2\mathbf{u} \cdot \mathbf{v}\right] d\mathbf{x} = \int_\Omega \mathbf{j} \cdot \mathbf{v}\, d\mathbf{x} \tag{1.2}$$

* Department of Mathematics, University of Leicester, Leicester LE1 7RH, England, email: Paul.Houston@mcs.le.ac.uk. Supported by the EPSRC (Grant GR/R76615).

† Dipartimento di Matematica, Università di Pavia, Via Ferrata 1, 27100 Pavia, Italy, email: perugia@dimat.unipv.it.

‡ Department of Mathematics, University of Basel, Rheinsprung 21, 4051 Basel, Switzerland, email: schneeba@math.unibas.ch. Supported by the Swiss National Science Foundation under project 21-068126.02.

§ Mathematics Department, University of British Columbia, 121-1984 Mathematics Road, Vancouver V6T 1Z2, Canada, email: schoetzau@math.ubc.ca.

for all $\mathbf{v} \in H_0(\mathrm{curl};\Omega)$. Under the assumption that k^2 is *not* a Maxwell eigenvalue, problem (1.2) is uniquely solvable; see, e.g., [19, Chapter 4] or [12, Section 5] for details.

The main motivation for using a discontinuous Galerkin approach for the numerical approximation of the above problem is that DG methods, being based on discontinuous finite element spaces, can easily handle meshes with hanging nodes and and local spaces of different orders. This renders DG methods ideally suited for *hp*–adaptive algorithms. Moreover, the implementation of discontinuous elements can be based on standard shape functions - a convenience that is particularly advantageous for high-order elements and that is not straightforwardly shared by standard edge or face elements commonly used in computational electromagnetics (see [9, 25, 1] and the references therein for *hp*-adaptive edge element methods).

This paper is a continuation of a series of papers that has been concerned with the development of DG finite element methods for the numerical approximation of the time-harmonic Maxwell equations. Indeed, in [22] an *hp*–local discontinuous Galerkin method was presented for the *low-frequency* approximation of these equations in heterogeneous media. The focus there was on the problem of how to discretize the curl-curl operator using discontinuous finite element spaces. The numerical experiments presented in [15] confirmed the expected *hp*–convergence rates, and indicate that DG methods can indeed be effective in a wide range of low-frequency applications with *coercive* bilinear forms. Then, in [23], [13], and [16], several *mixed* DG formulations were studied for the discretization of the time-harmonic Maxwell equations in mixed form. The mixed form was chosen to provide control on the divergence of the electric field and arises naturally in certain types of low-frequency models. In particular, it was shown that divergence constraints can be successfully incorporated within the DG framework by means of suitable Lagrange multipliers. Finally, we mention the recent work of [11] where extensive computational studies of DG discretizations applied to Maxwell eigenvalue problems can be found.

In this paper, we present the *first* numerical analysis of the interior penalty method applied to Maxwell equations in the non-mixed form (1.1). We show that the error in the DG energy norm converges with the optimal order $\mathcal{O}(h^{\min\{s,\ell\}})$ with respect to the mesh size h, the polynomial degree ℓ, and the regularity exponent s of the analytical solution. Under additional regularity assumptions, we further prove that the error in the L^2-norm converges with the full order $\mathcal{O}(h^{\ell+1})$. The derivation of these bounds relies on two crucial technical ingredients: the first one is that, as for conforming discretizations, the error between the analytical solution and its interior penalty approximation is *discretely divergence-free*. The second ingredient is an approximation property that ensures the existence of a conforming finite element function close to any discontinuous one and allows us to control the non-conformity of the method. This approximation property is established using the techniques in [13, 16] for the analysis of mixed DG methods and in [17] for the study of a-posteriori error estimation for DG discretizations of diffusion problems. Invoking these auxiliary results, the energy error bound is then derived by suitably modifying the argument in [20] and [19, Section 7.2], while the L^2-error bound is obtained along the lines of the proof of [18, Theorem 3.2], adapted to Nédélec's elements of second type. Our error bounds and the performance of the proposed method are tested in a series of numerical examples in two dimensions.

We note that, being based on duality techniques, the analysis in this paper does not cover the case of non-smooth material coefficients. This is in contrast to the recent techniques developed for conforming methods that allow for non-smooth coefficients. We mention here [5], where the analysis relies on the uniform convergence of the Maxwell resolvent operator and on the abstract theory of [6] for the approximation of nonlinear problems, and [12, 7] (see also [8]), where the analysis is based on the theory of compactly perturbed linear operators and on uniformly stable discrete Helmholtz decompositions. The extension of the results in this paper to problems with non-smooth coefficients remains an open problem. On the other hand, it is our belief that the recent results obtained in [16] for mixed DG discretizations of the Maxwell operator, combined with some of the technical results established in this paper might be useful in this direction.

The outline of the paper is as follows. In Section 2, we introduce the interior penalty DG method for the discretization of (1.1). Our main results are the optimal a-priori error bounds stated and discussed in Section 3. These results are proved in Sections 4 through 6 and numerically confirmed in the tests presented in Section 7. In Section 8, we end our presentation with concluding remarks. The Appendix contains a complete proof of an approximation result that plays a crucial role in our analysis.

Notation. For a bounded domain D in $\mathbb{R}^2$ or $\mathbb{R}^3$, we denote by $H^s(D)$ the standard Sobolev space of functions with regularity exponent $s \geq 0$, and norm $\|\cdot\|_{s,D}$. When $D = \Omega$, we simply write $\|\cdot\|_s$. For $s = 0$, we write $L^2(D)$ in lieu of $H^0(D)$. We also write $\|\cdot\|_{s,D}$ to denote the norm for the space $H^s(D)^d$, $d = 2, 3$. $H_0^1(D)$ is the subspace of $H^1(D)$ of functions with zero trace on ∂D. On the computational domain Ω, we further introduce the spaces

$$H(\mathrm{curl};\Omega) := \{\, \mathbf{v} \in L^2(\Omega)^3 : \nabla \times \mathbf{v} \in L^2(\Omega)^3 \,\},$$
$$H(\mathrm{div};\Omega) := \{\, \mathbf{v} \in L^2(\Omega)^3 : \nabla \cdot \mathbf{v} \in L^2(\Omega) \,\},$$

with the norms $\|\mathbf{v}\|_{\mathrm{curl}}^2 := \|\mathbf{v}\|_0^2 + \|\nabla\times\mathbf{v}\|_0^2$ and $\|\mathbf{v}\|_{\mathrm{div}}^2 := \|\mathbf{v}\|_0^2 + \|\nabla\cdot\mathbf{v}\|_0^2$, respectively. We denote by $H_0(\mathrm{curl};\Omega)$ the subspace of $H(\mathrm{curl};\Omega)$ of functions with zero tangential trace, and by $H(\mathrm{div}^0;\Omega)$ the subspace of $H(\mathrm{div};\Omega)$ of divergence-free functions. Finally, $(\cdot,\cdot)$ denotes the standard inner product in $L^2(\Omega)^3$ given by $(\mathbf{u},\mathbf{v}) := \int_\Omega \mathbf{u}\cdot\mathbf{v}\, d\mathbf{x}$.

2. Discontinuous Galerkin discretization. In this section, we introduce the interior penalty DG discretization of (1.1). To this end, we define the following notation. We consider shape-regular affine meshes $\mathcal{T}_h$ that partition the domain Ω into tetrahedra $\{K\}$; the parameter h denotes the mesh size of $\mathcal{T}_h$ given by $h = \max_{K\in\mathcal{T}_h} h_K$, where h_K is the diameter of the element $K \in \mathcal{T}_h$. We denote by $\mathcal{F}_h^{\mathcal{I}}$ the set of all interior faces of elements in $\mathcal{T}_h$, by $\mathcal{F}_h^{\mathcal{B}}$ the set of all boundary faces, and set $\mathcal{F}_h := \mathcal{F}_h^{\mathcal{I}} \cup \mathcal{F}_h^{\mathcal{B}}$. For a piecewise smooth vector-valued function $\mathbf{v}$, we introduce the following trace operators. Let $f \in \mathcal{F}_h^{\mathcal{I}}$ be an interior face shared by two neighboring elements K^+ and K^-; we write $\mathbf{n}^\pm$ to denote the unit outward normal vectors on the boundaries $\partial K^\pm$, respectively. Denoting by $\mathbf{v}^\pm$ the traces of $\mathbf{v}$ taken from within $K^\pm$, respectively, we define the tangential jumps and averages across f by

$$[\![\mathbf{v}]\!]_T := \mathbf{n}^+ \times \mathbf{v}^+ + \mathbf{n}^- \times \mathbf{v}^-, \qquad \{\!\{\mathbf{v}\}\!\} := (\mathbf{v}^+ + \mathbf{v}^-)/2,$$

respectively. On a boundary face $f \in \mathcal{F}_h^{\mathcal{B}}$, we set $[\![\mathbf{v}]\!]_T := \mathbf{n} \times \mathbf{v}$ and $\{\!\{\mathbf{v}\}\!\} := \mathbf{v}$.

For a given partition $\mathcal{T}_h$ of Ω and an approximation order $\ell \geq 1$, we wish to approximate the time-harmonic Maxwell equations (1.1) in the finite element space

$$\mathbf{V}_h := \{\mathbf{v} \in L^2(\Omega)^3 : \mathbf{v}|_K \in \mathcal{P}^\ell(K)^3 \ \ \forall K \in \mathcal{T}_h\}, \tag{2.1}$$

where $\mathcal{P}^\ell(K)$ denotes the space of polynomials of total degree at most ℓ on K.

Thereby, we consider the DG method: find $\mathbf{u}_h \in \mathbf{V}_h$ such that

$$a_h(\mathbf{u}_h, \mathbf{v}) = (\mathbf{j}, \mathbf{v}) \tag{2.2}$$

for all $\mathbf{v} \in \mathbf{V}_h$. The discrete form $a_h(\cdot,\cdot)$ is given by

$$\begin{aligned} a_h(\mathbf{u},\mathbf{v}) :=& (\nabla_h \times \mathbf{u}, \nabla_h \times \mathbf{v}) - k^2(\mathbf{u},\mathbf{v}) - \int_{\mathcal{F}_h} [\![\mathbf{u}]\!]_T \cdot \{\!\{\nabla_h \times \mathbf{v}\}\!\}\, ds \\ & - \int_{\mathcal{F}_h} [\![\mathbf{v}]\!]_T \cdot \{\!\{\nabla_h \times \mathbf{u}\}\!\}\, ds + \int_{\mathcal{F}_h} \mathtt{a}\, [\![\mathbf{u}]\!]_T \cdot [\![\mathbf{v}]\!]_T\, ds. \end{aligned} \tag{2.3}$$

Here, we use ∇_h to denote the elementwise application of the operator ∇. Further, we use the notation $\int_{\mathcal{F}_h} \varphi\, ds := \sum_{f\in\mathcal{F}_h} \int_f \varphi\, ds$. The function $\mathtt{a} \in L^\infty(\mathcal{F}_h)$ is the *interior penalty* stabilization function. To define it, we first introduce $\mathtt{h}$ in $L^\infty(\mathcal{F}_h)$ as

$$\mathtt{h}(\mathbf{x}) := h_f, \qquad \mathbf{x} \in f,\ f \in \mathcal{F}_h,$$

with h_f denoting the diameter of face f. Then we set

$$\mathtt{a} := \alpha\, \mathtt{h}^{-1}, \tag{2.4}$$

where α is a positive parameter independent of the mesh size and the wave number.

3. A-priori error bounds. In this section, we state our main results, namely optimal a-priori error bounds for the DG method (2.2) with respect to a (broken) energy norm and the L^2-norm.

3.1. Gårding inequality. Before stating the error bounds, we need to establish a Gårding-type stability result for the form $a_h(\cdot,\cdot)$. To this end, we set

$$\mathbf{V}(h) := H_0(\mathrm{curl};\Omega) + \mathbf{V}_h,$$

and define the following DG seminorm and norm on $\mathbf{V}(h)$, respectively:

$$|\mathbf{v}|_{DG}^2 := \|\nabla_h \times \mathbf{v}\|_0^2 + \|\mathtt{h}^{-\frac{1}{2}}[\![\mathbf{v}]\!]_T\|_{0,\mathcal{F}_h}^2, \qquad \|\mathbf{v}\|_{DG}^2 := \|\mathbf{v}\|_0^2 + |\mathbf{v}|_{DG}^2.$$

Here, we write $\|\varphi\|_{0,\mathcal{F}_h}^2 := \sum_{f\in\mathcal{F}_h} \|\varphi\|_{0,f}^2$. The norm $\|\cdot\|_{DG}$ can be viewed as the *energy* norm for the discretization under consideration. With this notation, the following Gårding inequality holds.

LEMMA 3.1. *There exists a parameter $\alpha_{\min} > 0$, independent of the mesh size and the wave number, such that for $\alpha \geq \alpha_{\min}$ we have*

$$a_h(\mathbf{v},\mathbf{v}) \geq \beta \|\mathbf{v}\|_{DG}^2 - (k^2+\beta)\|\mathbf{v}\|_0^2 \quad \textit{for all} \quad \mathbf{v} \in \mathbf{V}_h,$$

with a constant $\beta > 0$ independent of the mesh size and the wave number.

Proof. Using standard inverse estimates, it can be readily seen that there is a parameter $\alpha_{\min} > 0$ such that for $\alpha \geq \alpha_{\min}$ we have

$$a_h(\mathbf{v},\mathbf{v}) \geq \beta |\mathbf{v}|_{DG}^2 - k^2\|\mathbf{v}\|_0^2 \quad \text{for all} \quad \mathbf{v} \in \mathbf{V}_h,$$

for a constant $\beta > 0$ independent of the mesh size; we refer to [4, 15, 23] for details. The result of the lemma now follows immediately. ☐

The condition $\alpha \geq \alpha_{\min} > 0$ is a restriction that is typical for interior penalty methods and may be omitted by using other DG discretizations of the curl-curl operator, such as the non-symmetric interior penalty or the LDG method; see, e.g., [4, 22] for details.

3.2. Energy error. We are now ready to state and discuss the following a-priori bound for the error in the energy norm $\|\cdot\|_{DG}$; the detailed proof will be carried out in Section 5.

THEOREM 3.2. *Assume that the analytical solution* $\mathbf{u}$ *of (1.1) satisfies the regularity assumption*

$$\mathbf{u} \in H^s(\Omega)^3, \qquad \nabla \times \mathbf{u} \in H^s(\Omega)^3, \tag{3.1}$$

for $s > \frac{1}{2}$. *Furthermore, let* $\mathbf{u}_h$ *denote the DG approximation defined by (2.2) with* $\alpha \geq \alpha_{\min}$. *Then there is a mesh size* $h_0 > 0$ *such that for* $0 < h \leq h_0$, *we have the optimal a priori error bound*

$$\|\mathbf{u} - \mathbf{u}_h\|_{DG} \leq C\, h^{\min\{s,\ell\}} \Big[\|\mathbf{u}\|_s + \|\nabla \times \mathbf{u}\|_s \Big],$$

with a constant $C > 0$ *independent of the mesh size.*

REMARK 3.3. *For a source term* $\mathbf{j} \in H(\mathrm{div};\Omega)$, *the regularity assumption in (3.1) is ensured by the embedding results in [3, Proposition 3.7]; see also (3.2) below. In particular, assumption (3.1) is satisfied in the physically most relevant case of a solenoidal forcing term where* $\nabla \cdot \mathbf{j} = 0$. *In this sense, the smoothness requirement in (3.1) is minimal.*

Proceeding along the lines of [24], we conclude from the a-priori error bound in Theorem 3.2 the existence and uniqueness of discrete solutions.

COROLLARY 3.4. *For a stabilization parameter* $\alpha \geq \alpha_{\min}$, *the DG method (2.2) admits a unique solution* $\mathbf{u}_h \in \mathbf{V}_h$, *provided that* $h \leq h_0$.

Proof. We only need to establish that if $\mathbf{j} = \mathbf{0}$, then the only solution to (2.2) is $\mathbf{u}_h = \mathbf{0}$. In fact, if $\mathbf{j} = \mathbf{0}$, then $\mathbf{u} = \mathbf{0}$, and the estimate of Theorem 3.2 implies $\|\mathbf{u}_h\|_{DG} \leq 0$, thereby $\mathbf{u}_h = \mathbf{0}$, for $h \leq h_0$. □

3.3. Error in $\mathbf{L}^2(\boldsymbol{\Omega})^3$. Next, we state an a-priori bound for the error $\|\mathbf{u} - \mathbf{u}_h\|_0$ and show that the optimal order $\mathcal{O}(h^{\ell+1})$ is obtained for smooth solutions and convex domains. To this end, we will use the following embedding from [3, Proposition 3.7]: under the foregoing assumptions on the domain Ω, there exists a regularity exponent $\sigma \in (1/2, 1]$, depending only on Ω, such that

$$\begin{aligned} &H_0(\mathrm{curl};\Omega) \cap H(\mathrm{div};\Omega) \hookrightarrow H^\sigma(\Omega)^3, \\ &H(\mathrm{curl};\Omega) \cap H_0(\mathrm{div};\Omega) \hookrightarrow H^\sigma(\Omega)^3. \end{aligned} \tag{3.2}$$

The maximal value of σ for which the above embedding holds is closely related to the regularity properties of the Laplacian in polyhedra and only depends on the opening angles at the corners and edges of the domain, cf. [3]. In particular, for a convex domain, (3.2) holds with $\sigma = 1$.

Furthermore, let us denote by $\boldsymbol{\Pi}_{\mathrm{N}}$ the curl-conforming Nédéléc interpolation operator of the second kind into $\mathbf{V}_h \cap H_0(\mathrm{curl};\Omega)$; see [21] or [19, Section 8.2]. Then, we have the following result.

THEOREM 3.5. *Let* $\mathbf{u}$ *denote the analytical solution of (1.1) and* $\mathbf{u}_h$ *the DG approximation obtained by (2.2) with* $\alpha \geq \alpha_{\min}$. *Then there is a mesh size* $h_1 > 0$ *such that for* $0 < h \leq h_1$ *we have*

$$\|\mathbf{u} - \mathbf{u}_h\|_0 \leq Ch^\sigma \|\mathbf{u} - \mathbf{u}_h\|_{DG} + Ch^\sigma \|\mathbf{u} - \boldsymbol{\Pi}_{\mathrm{N}}\mathbf{u}\|_{\mathrm{curl}} + C\|\mathbf{u} - \boldsymbol{\Pi}_{\mathrm{N}}\mathbf{u}\|_0,$$

with a constant $C > 0$ *independent of the mesh size. The parameter* $\sigma \in (1/2, 1]$ *is the embedding exponent from (3.2).*

Under additional smoothness assumptions on the analytical solution $\mathbf{u}$, the bound in Theorem 3.5 combined with the approximation properties for $\mathbf{\Pi}_{\mathrm{N}}$ and the error estimate in Theorem 3.2 result in the following L^2-error bound:

COROLLARY 3.6. *Assume that the analytical solution* $\mathbf{u}$ *of (1.1) satisfies the regularity assumption*

$$\mathbf{u} \in H^{s+\sigma}(\Omega)^3, \qquad \nabla \times \mathbf{u} \in H^s(\Omega)^3, \tag{3.3}$$

for $s > \frac{1}{2}$ *and the parameter* σ *from (3.2). Let* $\mathbf{u}_h$ *denote the DG approximation obtained by (2.2) with* $\alpha \geq \alpha_{\min}$. *Then there is a mesh size* $h_2 > 0$ *such that for* $0 < h \leq h_2$ *we have the a-priori error bound*

$$\|\mathbf{u} - \mathbf{u}_h\|_0 \leq C\, h^{\min\{s,\ell\}+\sigma} \Big[\|\mathbf{u}\|_{s+\sigma} + \|\nabla \times \mathbf{u}\|_s\Big],$$

with a constant $C > 0$ *independent of the mesh size* h.

REMARK 3.7. *In particular, for a convex domain where* $\sigma = 1$ *and an analytical solution* $\mathbf{u} \in H^{\ell+1}(\Omega)^3$, *Corollary 3.6 ensures the optimal error bound*

$$\|\mathbf{u} - \mathbf{u}_h\|_0 \leq C h^{\ell+1} \|\mathbf{u}\|_{\ell+1},$$

holds, with a constant $C > 0$ *independent of the mesh size.*

The detailed proofs of Theorem 3.5 and Corollary 3.6 can be found in Section 6.

4. Auxiliary results. This section is devoted to the collection of some auxiliary results which will be required throughout the rest of this article. In Section 4.1 and Section 4.2, we start by recalling some well-known facts from the finite element theory of Maxwell's equations; see, e.g., [12, 19] and the references cited therein. Then, in Section 4.3, we present novel approximation results that allow us to control the non-conformity of the interior penalty method. Note that similar approximation techniques have been used in [13, 16] for the analysis of mixed DG methods and in [17] for the derivation of a-posteriori error bounds for DG discretizations of diffusion problems. In Section 4.4, we rewrite the interior penalty method (2.2) in a perturbed form and establish crucial properties of this auxiliary formulation. In particular, we show that the error $\mathbf{u} - \mathbf{u}_h$ is discretely divergence-free.

4.1. Helmholtz decompositions. We begin by recalling the subsequent continuous Helmholtz decomposition: under the foregoing assumptions on the domain, we have

$$L^2(\Omega)^3 = H(\mathrm{div}^0; \Omega) \oplus \nabla H_0^1(\Omega); \tag{4.1}$$

the decomposition being orthogonal in $L^2(\Omega)^3$; see, e.g., [10, Section 4].

A similar decomposition holds on the discrete level. To this end, we define $\mathbf{V}_h^c$ to be the largest conforming space underlying $\mathbf{V}_h$, that is,

$$\mathbf{V}_h^c := \mathbf{V}_h \cap H_0(\mathrm{curl}; \Omega). \tag{4.2}$$

In fact, $\mathbf{V}_h^c$ is Nédélec's space of the second kind; see [21] or [19, Section 8.2]. The space $\mathbf{V}_h^c$ can then be decomposed into

$$\mathbf{V}_h^c = \mathbf{X}_h \oplus \nabla S_h, \tag{4.3}$$

with the spaces S_h and $\mathbf{X}_h$ given by

$$S_h := \{\, q \in H^1_0(\Omega) : q|_K \in \mathcal{P}^{\ell+1}(K),\ K \in \mathcal{T}_h\}, \tag{4.4}$$
$$\mathbf{X}_h := \{\mathbf{v} \in \mathbf{V}^c_h : (\mathbf{v}, \nabla q) = 0\ \forall q \in S_h\}, \tag{4.5}$$

respectively. The space $\mathbf{X}_h$ is referred to as the space of *discretely divergence-free* functions. By construction, the decomposition (4.3) is orthogonal in $L^2(\Omega)^3$; cf. [19, Section 8.2].

4.2. Standard approximation operators. Next, we introduce standard approximation operators and state their properties. We start by recalling the properties of the curl-conforming Nédélec interpolant $\mathbf{\Pi}_{\mathrm{N}}$ of the second kind.

LEMMA 4.1. *There exists a positive constant C, independent of the mesh size, such that, for any $\mathbf{v} \in H_0(\mathrm{curl};\Omega) \cap H^t(\Omega)^3$ with $\nabla\times\mathbf{v} \in H^t(\Omega)^3$, $t > \frac{1}{2}$,*

$$\|\mathbf{v} - \mathbf{\Pi}_{\mathrm{N}}\mathbf{v}\|_{\mathrm{curl}} \le C\, h^{\min\{t,\ell\}}\big[\|\mathbf{v}\|_t + \|\nabla\times\mathbf{v}\|_t\big], \tag{4.6}$$
$$\|\nabla\times(\mathbf{v} - \mathbf{\Pi}_{\mathrm{N}}\mathbf{v})\|_0 \le C\, h^{\min\{t,\ell\}}\|\nabla\times\mathbf{v}\|_t. \tag{4.7}$$

Moreover, there exists a positive constant C, independent of the mesh size, such that, for any $\mathbf{v} \in H_0(\mathrm{curl};\Omega) \cap H^{1+t}(\Omega)^3$ with $t > 0$,

$$\|\mathbf{v} - \mathbf{\Pi}_{\mathrm{N}}\mathbf{v}\|_0 \le C\, h^{\min\{t,\ell\}+1}\|\mathbf{v}\|_{1+t}. \tag{4.8}$$

Proof. A proof of the first two results can be found in [19, Theorem 5.41, Remark 5.42 and Theorem 8.15].

To prove (4.8), we first consider the case $t \in (0,1)$ and establish the corresponding estimate on the reference tetrahedron $\widehat{K}$. From the stability of the Nédélec interpolation operator $\widehat{\mathbf{\Pi}}_{\mathrm{N}}$ in $W^{1,p}(\widehat{K})^3$ for any $p > 2$ (see [19, Lemma 5.38], [18], and references therein) and the embedding $H^{1+t}(\widehat{K})^3 \hookrightarrow W^{1,p}(\widehat{K})^3$ for $p = \frac{6}{3-2t}$ (see, e.g., [19, Theorem 3.7]), we conclude that

$$\begin{aligned}\|\widehat{\mathbf{v}} - \widehat{\mathbf{\Pi}}_{\mathrm{N}}\widehat{\mathbf{v}}\|_{0,\widehat{K}} &\le \inf_{\widehat{\mathbf{q}}\in\mathcal{P}^\ell(\widehat{K})^3}\Big\{\|\widehat{\mathbf{v}} - \widehat{\mathbf{q}}\|_{0,\widehat{K}} + \|\widehat{\mathbf{\Pi}}_{\mathrm{N}}\,(\widehat{\mathbf{v}} - \widehat{\mathbf{q}})\,\|_{0,\widehat{K}}\Big\}\\ &\le C \inf_{\widehat{\mathbf{q}}\in\mathcal{P}^\ell(\widehat{K})^3}\|\widehat{\mathbf{v}} - \widehat{\mathbf{q}}\|_{W^{1,p}(\widehat{K})} \le C \inf_{\widehat{\mathbf{q}}\in\mathcal{P}^\ell(\widehat{K})^3}\|\widehat{\mathbf{v}} - \widehat{\mathbf{q}}\|_{1+t,\widehat{K}}.\end{aligned}$$

By a Bramble-Hilbert argument for fractional order Sobolev spaces, we therefore obtain

$$\|\widehat{\mathbf{v}} - \widehat{\mathbf{\Pi}}_{\mathrm{N}}\widehat{\mathbf{v}}\|_{0,\widehat{K}} \le C\,|\widehat{\mathbf{v}}|_{t+1,\widehat{K}}. \tag{4.9}$$

The bound in (4.8) follows then from (4.9) by a scaling argument. The proof for $t \ge 1$ is carried out similarly, using the H^2–stability of $\mathbf{\Pi}_{\mathrm{N}}$; see [21]. □

Furthermore, for any $\mathbf{v} \in H_0(\mathrm{curl};\Omega)$, we define the projection $\mathbf{\Pi}^c\mathbf{v} \in \mathbf{V}^c_h$ by

$$(\nabla\times(\mathbf{v} - \mathbf{\Pi}^c\mathbf{v}), \nabla\times\mathbf{w}) + (\mathbf{v} - \mathbf{\Pi}^c\mathbf{v}, \mathbf{w}) = 0 \qquad \forall \mathbf{w} \in \mathbf{V}^c_h. \tag{4.10}$$

An immediate consequence of this definition is that

$$\|\mathbf{v} - \mathbf{\Pi}^c\mathbf{v}\|_{\mathrm{curl}} = \inf_{\mathbf{w}\in\mathbf{V}^c_h}\|\mathbf{v} - \mathbf{w}\|_{\mathrm{curl}}.$$

Thus, from property (4.6) in Lemma 4.1 we obtain the following approximation result.

LEMMA 4.2. *There exists a positive constant C, independent of the mesh size, such that, for any $\mathbf{v} \in H_0(\mathrm{curl};\Omega) \cap H^t(\Omega)^3$ with $\nabla \times \mathbf{v} \in H^t(\Omega)^3$, $t > \frac{1}{2}$,*

$$\|\mathbf{v} - \mathbf{\Pi}^c\mathbf{v}\|_{\mathrm{curl}} \leq C\, h^{\min\{t,\ell\}} \big[\|\mathbf{v}\|_t + \|\nabla \times \mathbf{v}\|_t\big].$$

Next, let us denote by $\mathbf{\Pi}_h$ the L^2-projection onto $\mathbf{V}_h$. The following approximation result is well-known.

LEMMA 4.3. *There exists a positive constant C, independent of the local mesh sizes h_K, such that, for any $\mathbf{v} \in H^t(K)^3$, $K \in \mathcal{T}_h$, $t > \frac{1}{2}$,*

$$\|\mathbf{v} - \mathbf{\Pi}_h\mathbf{v}\|_{0,K}^2 + h_K\|\mathbf{v} - \mathbf{\Pi}_h\mathbf{v}\|_{0,\partial K}^2 \leq C\, h_K^{2t}\, \|\mathbf{v}\|_{t,K}^2.$$

Finally, we recall the following result that allows us to approximate discretely divergence-free functions by exactly divergence-free ones.

LEMMA 4.4. *For any discretely divergence-free function $\mathbf{v} \in \mathbf{X}_h$, define $\mathbf{H}\mathbf{v} \in H_0(\mathrm{curl};\Omega) \cap H(\mathrm{div}^0;\Omega)$ by $\nabla \times \mathbf{H}\mathbf{v} = \nabla \times \mathbf{v}$. Then, there exists a constant $C > 0$ such that*

$$\|\mathbf{v} - \mathbf{H}\mathbf{v}\|_0 \leq Ch^\sigma \|\nabla \times \mathbf{v}\|_0,$$

with the parameter σ from (3.2). Moreover, there holds $\|\mathbf{H}\mathbf{v}\|_0 \leq \|\mathbf{v}\|_0$.

The result in Lemma 4.4 is obtained by proceeding as in [12, Lemma 4.5] and [19, Lemma 7.6] using Nédélec's second family of elements. The L^2-stability of $\mathbf{H}$ is a consequence of the L^2-orthogonality of the continuous Helmholtz decomposition.

4.3. Conforming approximation of discontinuous functions. The following approximation result is instrumental in our analysis; it allows us to find a conforming finite element function close to any discontinuous one. This result is obtained by using the same techniques as those in [17, Section 2.1] and [16, Appendix]. As its proof is rather lengthy and technical, it is relegated to the Appendix.

PROPOSITION 4.5. *Let $\mathbf{v} \in \mathbf{V}_h$. Then there is a function $\mathbf{v}^c \in \mathbf{V}_h^c$ such that*

$$\|\mathbf{v} - \mathbf{v}^c\|_0^2 \leq C \int_{\mathcal{F}_h} \mathtt{h} |[\![\mathbf{v}]\!]_T|^2\, ds,$$

$$\|\mathbf{v} - \mathbf{v}^c\|_{DG}^2 \leq C \int_{\mathcal{F}_h} \mathtt{h}^{-1} |[\![\mathbf{v}]\!]_T|^2\, ds,$$

with a constant $C > 0$ independent of the mesh size.

Proposition 4.5 and the definition of the norm $\|\cdot\|_{DG}$ immediately imply the following result.

PROPOSITION 4.6. *Let $\mathbf{v} \in \mathbf{V}_h$. Then the conforming approximation $\mathbf{v}^c \in \mathbf{V}_h^c$ from Proposition 4.5 satisfies*

$$\|\mathbf{v} - \mathbf{v}^c\|_{DG} + \|\mathbf{v}^c\|_{DG} \leq C\|\mathbf{v}\|_{DG},$$

$$\|\mathbf{v} - \mathbf{v}^c\|_0 \leq Ch\|\mathbf{v}\|_{DG},$$

with a constant $C > 0$ independent of the mesh size.

We will further need the following consequence of Proposition 4.5, which follows from the fact that $[\![\mathbf{w}]\!]_T = \mathbf{0}$ on $\mathcal{F}_h$, for any $\mathbf{w} \in H_0(\mathrm{curl};\Omega)$, and the definition of the norm $\|\cdot\|_{DG}$.

PROPOSITION 4.7. *Let* $\mathbf{v} \in \mathbf{V}_h$ *and* $\mathbf{w} \in H_0(\mathrm{curl};\Omega)$. *Let* $\mathbf{v}^c \in \mathbf{V}_h^c$ *be the conforming approximation of* $\mathbf{v}$ *from Proposition 4.5. Then we have*

$$\|\mathbf{v}-\mathbf{v}^c\|_{DG} \le C\|\mathbf{v}-\mathbf{w}\|_{DG},$$
$$\|\mathbf{v}-\mathbf{v}^c\|_0 \le Ch\|\mathbf{v}-\mathbf{w}\|_{DG},$$

with a constant $C>0$ *independent of the mesh size.*

4.4. Perturbed formulation. Following [4], we rewrite the method (2.2) in a slightly perturbed form. To this end, we define for $\mathbf{v} \in \mathbf{V}(h)$ the lifting $\mathcal{L}(\mathbf{v}) \in \mathbf{V}_h$ by

$$(\mathcal{L}(\mathbf{v}),\mathbf{w}) = \int_{\mathcal{F}_h} [\![\mathbf{v}]\!]_T \cdot \{\!\{\mathbf{w}\}\!\}\, ds \qquad \forall \mathbf{w} \in \mathbf{V}_h. \tag{4.11}$$

Then we introduce the form

$$\begin{aligned}\widetilde{a}_h(\mathbf{u},\mathbf{v}) := (\nabla_h \times \mathbf{u}, \nabla_h \times \mathbf{v}) - k^2(\mathbf{u},\mathbf{v}) - (\mathcal{L}(\mathbf{u}), \nabla_h \times \mathbf{v})\\ -(\mathcal{L}(\mathbf{v}), \nabla_h \times \mathbf{u}) + \int_{\mathcal{F}_h} \mathtt{a}\,[\![\mathbf{u}]\!]_T \cdot [\![\mathbf{v}]\!]_T\, ds.\end{aligned}$$

Note that $a_h = \widetilde{a}_h$ in $\mathbf{V}_h \times \mathbf{V}_h$ although this is no longer true in $\mathbf{V}(h) \times \mathbf{V}(h)$. The discrete problem (2.2) can equivalently be formulated as: find $\mathbf{u}_h \in \mathbf{V}_h$ such that

$$\widetilde{a}_h(\mathbf{u}_h,\mathbf{v}) = (\mathbf{j},\mathbf{v}) \qquad \forall \mathbf{v} \in \mathbf{V}_h. \tag{4.12}$$

Next, let us establish some useful properties of the form $\widetilde{a}_h(\cdot,\cdot)$.

LEMMA 4.8. *There holds:*

(i) For $\mathbf{u},\mathbf{v} \in H_0(\mathrm{curl};\Omega)$, *we have*

$$\widetilde{a}_h(\mathbf{u},\mathbf{v}) = a(\mathbf{u},\mathbf{v}),$$

with the form $a(\cdot,\cdot)$ *defined in (1.2).*

(ii) There is a constant $\gamma>0$, *independent of the mesh size and the wave number, such that*

$$|\widetilde{a}_h(\mathbf{u},\mathbf{v})| \le (k^2+\gamma)\|\mathbf{u}\|_{DG}\|\mathbf{v}\|_{DG}$$

for all $\mathbf{u},\mathbf{v} \in \mathbf{V}(h)$.

Proof. The first property follows from the fact that for $\mathbf{w} \in H_0(\mathrm{curl};\Omega)$ we have $\mathcal{L}(\mathbf{w}) = \mathbf{0}$ and $[\![\mathbf{w}]\!]_T = \mathbf{0}$ on $\mathcal{F}_h$. To see the second property, we note that, by the definition of the interior penalty function $\mathtt{a}$ in (2.4), there is a continuity constant $\gamma>0$ such that

$$|\widetilde{a}_h(\mathbf{u},\mathbf{v})| \le \gamma|\mathbf{u}|_{DG}|\mathbf{v}|_{DG} + k^2\|\mathbf{u}\|_0\|\mathbf{v}\|_0;$$

see [22, Section 4] or [15, Proposition 1]. The claim now follows from the definition of the DG norm and the Cauchy-Schwarz inequality. ∎

For the analytical solution $\mathbf{u}$ of (1.1), we define the residual

$$r_h(\mathbf{u};\mathbf{v}) := \widetilde{a}_h(\mathbf{u},\mathbf{v}) - (\mathbf{j},\mathbf{v}), \qquad \mathbf{v} \in \mathbf{V}_h. \tag{4.13}$$

Thus, if $\mathbf{u}_h$ is the DG approximation in (2.2), we have the error equation

$$\widetilde{a}_h(\mathbf{u}-\mathbf{u}_h,\mathbf{v}) = r_h(\mathbf{u};\mathbf{v}) \tag{4.14}$$

for all $\mathbf{v} \in \mathbf{V}_h$.

LEMMA 4.9. *Let* $\mathbf{u}$ *be the analytical solution of (1.1). Then:*

(i) For $\mathbf{v} \in \mathbf{V}_h \cap H_0(\mathrm{curl};\Omega)$*, we have*

$$r_h(\mathbf{u};\mathbf{v}) = 0.$$

(ii) Additionally, let $\nabla \times \mathbf{u} \in H^s(\Omega)^3$ *for* $s > \frac{1}{2}$*. Then*

$$r_h(\mathbf{u};\mathbf{v}) = \int_{\mathcal{F}_h} [\![\mathbf{v}]\!]_T \cdot \{\!\{\nabla \times \mathbf{u} - \mathbf{\Pi}_h(\nabla \times \mathbf{u})\}\!\}\, ds, \qquad \mathbf{v} \in \mathbf{V}_h.$$

Moreover, there holds

$$|r_h(\mathbf{u};\mathbf{v})| \leq C h^{\min\{s,\ell\}} \|\mathbf{v}\|_{DG} \|\nabla \times \mathbf{u}\|_s,$$

where C *is a positive constant, independent of the mesh size.*

Proof. The first claim follows readily from property *(i)* in Lemma 4.8, equation (1.2) and the definition of $r_h(\cdot;\cdot)$. The residual expression in *(ii)* is obtained as in [22, Lemma 4.10] or [15, Proposition 2] using integration by parts, the definition of $\widetilde{a}_h(\cdot,\cdot)$ and $r_h(\cdot;\cdot)$, the defining properties of the L^2-projection $\mathbf{\Pi}_h$, and the differential equation (1.1). The desired bound for $|r_h(\mathbf{u};\mathbf{v})|$ follows with the weighted Cauchy-Schwarz inequality, the definition of $\|\cdot\|_{DG}$ and $\mathtt{a}$ in (2.4), and the approximation property in Lemma 4.3 for $\mathbf{\Pi}_h$. □

Finally, let us show that the error $\mathbf{u} - \mathbf{u}_h$ is discretely divergence-free in the following sense.

PROPOSITION 4.10. *Let* $\mathbf{u}$ *be the analytical solution of (1.1) and* $\mathbf{u}_h$ *the discontinuous Galerkin approximation obtained in (2.2). Then there holds*

$$(\mathbf{u} - \mathbf{u}_h, \nabla q) = 0 \qquad \forall q \in S_h,$$

with the space S_h *defined in (4.4).*

Proof. Note that, for $q \in S_h$, we have $\nabla q \in \mathbf{V}_h \cap H_0(\mathrm{curl};\Omega)$. Using the error equation (4.14) and property *(i)* of Lemma 4.9 gives

$$\widetilde{a}_h(\mathbf{u} - \mathbf{u}_h, \nabla q) = 0 \qquad \forall q \in S_h.$$

The definition of $\widetilde{a}_h(\cdot,\cdot)$, property *(i)* of Lemma 4.8, and the fact that $\nabla_h \times \nabla q = \mathbf{0}$ and $[\![\nabla q]\!]_T = \mathbf{0}$ on $\mathcal{F}_h$ result in

$$\widetilde{a}_h(\mathbf{u}_h, \nabla q) = -k^2(\mathbf{u}_h, \nabla q) \qquad \text{and} \qquad \widetilde{a}_h(\mathbf{u}, \nabla q) = a(\mathbf{u}, \nabla q) = -k^2(\mathbf{u}, \nabla q).$$

Thereby, the statement of the proposition follows directly. □

5. Proof of Theorem 3.2.

The proof of Theorem 3.2 essentially follows the approach given in [19, Section 7.2] and [20] for conforming finite elements, in combination with the crucial approximation results in Proposition 4.5.

5.1. A preliminary error bound.

In this section, we prove a preliminary error bound along the lines of [19, Lemma 7.5].

PROPOSITION 5.1. *Let* $\mathbf{u}$ *be the analytical solution of (1.1) and* $\mathbf{u}_h$ *the approximation obtained in (2.2) with* $\alpha \geq \alpha_{\min}$*. Then there holds*

$$\|\mathbf{u} - \mathbf{u}_h\|_{DG} \leq C\big[\inf_{\mathbf{v} \in \mathbf{V}_h} \|\mathbf{u} - \mathbf{v}\|_{DG} + \mathcal{R}_h(\mathbf{u}) + \mathcal{E}_h(\mathbf{u} - \mathbf{u}_h)\big],$$

with a constant $C > 0$ *independent of the mesh size. Here, we set*

$$\mathcal{R}_h(\mathbf{u}) := \sup_{\mathbf{0} \neq \mathbf{v} \in \mathbf{V}_h} \frac{r_h(\mathbf{u};\mathbf{v})}{\|\mathbf{v}\|_{DG}}, \qquad \mathcal{E}_h(\mathbf{u} - \mathbf{u}_h) := \sup_{\mathbf{0} \neq \mathbf{v} \in \mathbf{V}_h} \frac{|(\mathbf{u} - \mathbf{u}_h, \mathbf{v})|}{\|\mathbf{v}\|_{DG}}.$$

Proof. Let $\mathbf{v} \in \mathbf{V}_h$ be arbitrary. We first bound $\|\mathbf{v} - \mathbf{u}_h\|_{DG}$. Using the Gårding inequality in Lemma 3.1, the definition of $\widetilde{a}_h(\cdot,\cdot)$ and the error equation (4.14), we obtain

$$\begin{aligned}\beta\|\mathbf{v} - \mathbf{u}_h\|_{DG}^2 &\le a_h(\mathbf{v} - \mathbf{u}_h, \mathbf{v} - \mathbf{u}_h) + (k^2 + \beta)(\mathbf{v} - \mathbf{u}_h, \mathbf{v} - \mathbf{u}_h)\\ &= \widetilde{a}_h(\mathbf{v} - \mathbf{u}_h, \mathbf{v} - \mathbf{u}_h) + (k^2 + \beta)(\mathbf{v} - \mathbf{u}_h, \mathbf{v} - \mathbf{u}_h)\\ &= \widetilde{a}_h(\mathbf{v} - \mathbf{u}, \mathbf{v} - \mathbf{u}_h) + r_h(\mathbf{u}; \mathbf{v} - \mathbf{u}_h)\\ &\qquad +(k^2 + \beta)(\mathbf{v} - \mathbf{u}, \mathbf{v} - \mathbf{u}_h) + (k^2 + \beta)(\mathbf{u} - \mathbf{u}_h, \mathbf{v} - \mathbf{u}_h).\end{aligned}$$

From the continuity of $\widetilde{a}_h(\cdot,\cdot)$ in *(ii)* of Lemma 4.8 and the definition of $\mathcal{R}_h$ and $\mathcal{E}_h$, we conclude that

$$\begin{aligned}\|\mathbf{v} - \mathbf{u}_h\|_{DG} &\le \beta^{-1}\Big[(k^2 + \gamma)\|\mathbf{u} - \mathbf{v}\|_{DG} + \mathcal{R}_h(\mathbf{u})\\ &\qquad +(k^2 + \beta)\|\mathbf{u} - \mathbf{v}\|_{DG} + (k^2 + \beta)\mathcal{E}_h(\mathbf{u} - \mathbf{u}_h)\Big]\\ &\le C\Big[\|\mathbf{u} - \mathbf{v}\|_{DG} + \mathcal{R}_h(\mathbf{u}) + \mathcal{E}_h(\mathbf{u} - \mathbf{u}_h)\Big].\end{aligned}$$

Applying the triangle inequality gives

$$\begin{aligned}\|\mathbf{u} - \mathbf{u}_h\|_{DG} &\le \|\mathbf{u} - \mathbf{v}\|_{DG} + \|\mathbf{v} - \mathbf{u}_h\|_{DG}\\ &\le C\Big[\|\mathbf{u} - \mathbf{v}\|_{DG} + \mathcal{R}_h(\mathbf{u}) + \mathcal{E}_h(\mathbf{u} - \mathbf{u}_h)\Big].\end{aligned}$$

Taking the infimum over $\mathbf{v} \in \mathbf{V}_h$ gives the assertion. ◻

5.2. Estimate of $\mathcal{E}_h(\mathbf{u} - \mathbf{u}_h)$. Next, we estimate the error term $\mathcal{E}_h(\mathbf{u} - \mathbf{u}_h)$ defined in Proposition 5.1.

PROPOSITION 5.2. *There exists a positive constant C, independent of the mesh size, such that*

$$\mathcal{E}_h(\mathbf{u} - \mathbf{u}_h) \le Ch^{\sigma}\|\mathbf{u} - \mathbf{u}_h\|_{DG},$$

with the parameter $\sigma \in (1/2, 1]$ from (3.2).

Proof. Fix $\mathbf{v} \in \mathbf{V}_h$, and let $\mathbf{v}^c \in \mathbf{V}_h^c$ be the conforming approximation of $\mathbf{v}$ from Proposition 4.5. We bound $(\mathbf{u} - \mathbf{u}_h, \mathbf{v})$ in the following steps.

Step 1. Representation result: using the Helmholtz decomposition (4.3), we decompose $\mathbf{v}^c$ as

$$\mathbf{v}^c = \mathbf{v}_0^c \oplus \nabla r, \tag{5.1}$$

with $\mathbf{v}_0^c \in \mathbf{X}_h$ and $r \in S_h$. Employing (5.1), we obtain

$$\begin{aligned}(\mathbf{u} - \mathbf{u}_h, \mathbf{v}) &= (\mathbf{u} - \mathbf{u}_h, \mathbf{v} - \mathbf{v}^c) + (\mathbf{u} - \mathbf{u}_h, \mathbf{v}^c) = (\mathbf{u} - \mathbf{u}_h, \mathbf{v} - \mathbf{v}^c) + (\mathbf{u} - \mathbf{u}_h, \mathbf{v}_0^c)\\ &= (\mathbf{u} - \mathbf{u}_h, \mathbf{v} - \mathbf{v}^c) + (\mathbf{u} - \mathbf{u}_h, \mathbf{v}_0^c - \mathbf{H}\mathbf{v}_0^c) + (\mathbf{u} - \mathbf{u}_h, \mathbf{H}\mathbf{v}_0^c)\\ &\equiv T_1 + T_2 + T_3,\end{aligned}$$

with $\mathbf{H}\mathbf{v}_0^c$ from Lemma 4.4. Here, we have used the orthogonality property of the error $\mathbf{u} - \mathbf{u}_h$ in Proposition 4.10. It remains to bound the terms T_1, T_2 and T_3.

Step 2. Bound for T_1: the Cauchy-Schwarz inequality and the approximation result in Proposition 4.6 yields

$$|T_1| \le \|\mathbf{u} - \mathbf{u}_h\|_0\|\mathbf{v} - \mathbf{v}^c\|_0 \le Ch\|\mathbf{u} - \mathbf{u}_h\|_0\|\mathbf{v}\|_{DG}. \tag{5.2}$$

Step 3. Bound for T_2: using the Cauchy-Schwarz inequality and the approximation results in Lemma 4.4 and Proposition 4.6, we have

$$\begin{aligned}|T_2| &\leq \|\mathbf{u}-\mathbf{u}_h\|_0\|\mathbf{v}_0^c-\mathbf{H}\mathbf{v}_0^c\|_0 \leq Ch^\sigma\|\mathbf{u}-\mathbf{u}_h\|_0\|\nabla\times\mathbf{v}_0^c\|_0\\ &= Ch^\sigma\|\mathbf{u}-\mathbf{u}_h\|_0\|\nabla\times\mathbf{v}^c\|_0 \leq Ch^\sigma\|\mathbf{u}-\mathbf{u}_h\|_0\|\mathbf{v}^c\|_{DG}\\ &\leq Ch^\sigma\|\mathbf{u}-\mathbf{u}_h\|_0\|\mathbf{v}\|_{DG}.\end{aligned} \tag{5.3}$$

Step 4. Bound for T_3: to bound T_3, we use a duality approach. To this end, we set $\mathbf{w} := \mathbf{H}\mathbf{v}_0^c$ and let $\mathbf{z}$ denote the solution of the following problem:

$$\begin{aligned}\nabla\times\nabla\times\mathbf{z}-k^2\mathbf{z} &= \mathbf{w} && \text{in } \Omega,\\ \mathbf{n}\times\mathbf{z} &= \mathbf{0} && \text{on } \Gamma.\end{aligned} \tag{5.4}$$

Since $\mathbf{w}\in H(\mathrm{div}^0;\Omega)$, the solution $\mathbf{z}$ belongs to $H(\mathrm{div}^0;\Omega)$. As in [19, Lemma 7.7], we obtain from the embeddings in (3.2) that $\mathbf{z}\in H^\sigma(\Omega)^3$, $\nabla\times\mathbf{z}\in H^\sigma(\Omega)^3$ and

$$\|\mathbf{z}\|_\sigma + \|\nabla\times\mathbf{z}\|_\sigma \leq C\|\mathbf{w}\|_0, \tag{5.5}$$

for a stability constant $C>0$ and the parameter $\sigma\in(1/2,1]$ in (3.2).

Hence, multiplying the dual problem with $\mathbf{e}_h := \mathbf{u}-\mathbf{u}_h$ and integrating by parts, since $\nabla\times\mathbf{z}\in H(\mathrm{curl};\Omega)$, we obtain

$$\begin{aligned}(\mathbf{e}_h,\mathbf{w}) &= (\nabla\times\mathbf{z},\nabla_h\times\mathbf{e}_h)-k^2(\mathbf{z},\mathbf{e}_h)-\sum_{K\in\mathcal{T}_h}\int_{\partial K}\mathbf{n}_K\times\mathbf{e}_h\cdot\nabla\times\mathbf{z}\,ds\\ &= (\nabla\times\mathbf{z},\nabla_h\times\mathbf{e}_h)-k^2(\mathbf{z},\mathbf{e}_h)-\int_{\mathcal{F}_h}[\![\mathbf{e}_h]\!]_T\cdot\{\!\{\nabla\times\mathbf{z}\}\!\}\,ds.\end{aligned}$$

Let $\mathbf{z}_h = \mathbf{\Pi}_{\mathrm{N}}\mathbf{z}\in\mathbf{V}_h^c$ be the Nédélec interpolant of the second kind of $\mathbf{z}$ in (4.6) of Lemma 4.1, and $\mathbf{\Pi}_h$ the L^2–projection onto $\mathbf{V}_h$. Using the definition of $\widetilde{a}_h(\cdot,\cdot)$, the fact that $\mathbf{z}\in H_0(\mathrm{curl};\Omega)$, the error equation (4.14), property *(i)* of Lemma 4.9, and the definition of $\mathbf{\Pi}_h$ and $\mathcal{L}$, we obtain

$$\begin{aligned}(\mathbf{e}_h,\mathbf{w}) &= \widetilde{a}_h(\mathbf{e}_h,\mathbf{z})+(\mathcal{L}(\mathbf{e}_h),\nabla\times\mathbf{z})-\int_{\mathcal{F}_h}[\![\mathbf{e}_h]\!]_T\cdot\{\!\{\nabla\times\mathbf{z}\}\!\}\,ds\\ &= \widetilde{a}_h(\mathbf{e}_h,\mathbf{z}-\mathbf{z}_h)+(\mathcal{L}(\mathbf{e}_h),\mathbf{\Pi}_h(\nabla\times\mathbf{z}))-\int_{\mathcal{F}_h}[\![\mathbf{e}_h]\!]_T\cdot\{\!\{\nabla\times\mathbf{z}\}\!\}\,ds\\ &= \widetilde{a}_h(\mathbf{e}_h,\mathbf{z}-\mathbf{z}_h)-\int_{\mathcal{F}_h}[\![\mathbf{e}_h]\!]_T\cdot\{\!\{\nabla\times\mathbf{z}-\mathbf{\Pi}_h(\nabla\times\mathbf{z})\}\!\}\,ds.\end{aligned}$$

First, we note that, employing the weighted Cauchy-Schwarz inequality, the approximation properties in Lemma 4.3 and the stability bound (5.5), we get

$$\begin{aligned}&\left|\int_{\mathcal{F}_h}[\![\mathbf{e}_h]\!]_T\cdot\{\!\{\nabla\times\mathbf{z}-\mathbf{\Pi}_h(\nabla\times\mathbf{z})\}\!\}\,ds\right|\\ &\quad\leq C\left(\int_{\mathcal{F}_h}\mathrm{h}^{-1}|[\![\mathbf{e}_h]\!]_T|^2\,ds\right)^{\frac12}\left(\sum_{K\in\mathcal{T}_h}h_K\|\nabla\times\mathbf{z}-\mathbf{\Pi}_h(\nabla\times\mathbf{z})\|_{0,\partial K}^2\right)^{\frac12}\\ &\quad\leq Ch^\sigma\|\mathbf{e}_h\|_{DG}\|\nabla\times\mathbf{z}\|_\sigma \leq Ch^\sigma\|\mathbf{e}_h\|_{DG}\|\mathbf{w}\|_0.\end{aligned}$$

Furthermore, the continuity of $\widetilde{a}_h(\cdot,\cdot)$ in Lemma 4.8, the approximation property (4.6) in Lemma 4.1 and the stability estimate (5.5) yield

$$\widetilde{a}_h(\mathbf{e}_h, \mathbf{z}-\mathbf{z}_h) \leq Ch^\sigma \|\mathbf{e}_h\|_{DG} \|\mathbf{w}\|_0.$$

Combining the above bounds gives

$$(\mathbf{e}_h, \mathbf{w}) \leq Ch^\sigma \|\mathbf{e}_h\|_{DG} \|\mathbf{w}\|_0.$$

Since $\|\mathbf{w}\|_0 \leq \|\mathbf{v}_0^c\|_0 \leq \|\mathbf{v}^c\|_0 \leq C\|\mathbf{v}\|_{DG}$, in view of Lemma 4.4 and Proposition 4.6, we conclude that

$$|T_3| \leq Ch^\sigma \|\mathbf{u}-\mathbf{u}_h\|_{DG} \|\mathbf{v}\|_{DG}. \tag{5.6}$$

Step 5. Conclusion: referring to (5.2), (5.3) and (5.6) yields

$$|(\mathbf{u}-\mathbf{u}_h, \mathbf{v})| \leq Ch^\sigma \|\mathbf{u}-\mathbf{u}_h\|_{DG} \|\mathbf{v}\|_{DG},$$

from where the assertion follows. □

5.3. The error bound in Theorem 3.2. We are now ready to complete the proof of Theorem 3.2. From Proposition 5.1 and Proposition 5.2, we obtain

$$\begin{aligned}\|\mathbf{u}-\mathbf{u}_h\|_{DG} &\leq C\left[\inf_{\mathbf{v}\in\mathbf{V}_h} \|\mathbf{u}-\mathbf{v}\|_{DG} + \mathcal{R}_h(\mathbf{u}) + \mathcal{E}_h(\mathbf{u}-\mathbf{u}_h)\right] \\ &\leq C\left[\inf_{\mathbf{v}\in\mathbf{V}_h} \|\mathbf{u}-\mathbf{v}\|_{DG} + \mathcal{R}_h(\mathbf{u}) + h^\sigma \|\mathbf{u}-\mathbf{u}_h\|_{DG}\right]. \end{aligned} \tag{5.7}$$

Hence, if the mesh size is sufficiently small we can absorb the third term on the right-hand of (5.7) into the left-hand side; thereby,

$$\|\mathbf{u}-\mathbf{u}_h\|_{DG} \leq C\left[\inf_{\mathbf{v}\in\mathbf{V}_h} \|\mathbf{u}-\mathbf{v}\|_{DG} + \mathcal{R}_h(\mathbf{u})\right].$$

Choosing $\mathbf{v} = \mathbf{\Pi}_{\mathrm{N}}\mathbf{u}$, the Nédélec interpolant of $\mathbf{u}$, from the interpolation estimate (4.6) in Lemma 4.1 and the estimate of the residual in *(ii)* of Lemma 4.9 give the result in Theorem 3.2.

6. Proof of Theorem 3.5 and Corollary 3.6. In this section, we complete the proof of Theorem 3.5 and Corollary 3.6. Our analysis proceeds along the lines of [18, Section 4].

6.1. Proof of Theorem 3.5. In order to prove Theorem 3.5, let $\mathbf{u}_h^c \in \mathbf{V}_h^c$ be the conforming approximation of $\mathbf{u}_h$ from Proposition 4.5. We can write

$$\|\mathbf{u}-\mathbf{u}_h\|_0^2 = (\mathbf{u}-\mathbf{u}_h, \mathbf{u}-\mathbf{\Pi}_{\mathrm{N}}\mathbf{u}) + (\mathbf{u}-\mathbf{u}_h, \mathbf{\Pi}_{\mathrm{N}}\mathbf{u}-\mathbf{u}_h^c) + (\mathbf{u}-\mathbf{u}_h, \mathbf{u}_h^c-\mathbf{u}_h).$$

By using the Cauchy-Schwarz inequality and Proposition 4.7, we have

$$\|\mathbf{u}-\mathbf{u}_h\|_0 \leq \|\mathbf{u}-\mathbf{\Pi}_{\mathrm{N}}\mathbf{u}\|_0 + Ch\|\mathbf{u}-\mathbf{u}_h\|_{DG} + \frac{|(\mathbf{u}-\mathbf{u}_h, \mathbf{\Pi}_{\mathrm{N}}\mathbf{u}-\mathbf{u}_h^c)|}{\|\mathbf{u}-\mathbf{u}_h\|_0}, \tag{6.1}$$

with $C > 0$ independent of the mesh size. For the last term on the right-hand side of (6.1), we claim that, for a sufficiently small mesh size, there holds:

$$\frac{|(\mathbf{u}-\mathbf{u}_h, \mathbf{\Pi}_{\mathrm{N}}\mathbf{u}-\mathbf{u}_h^c)|}{\|\mathbf{u}-\mathbf{u}_h\|_0} \leq C\|\mathbf{u}-\mathbf{\Pi}_{\mathrm{N}}\mathbf{u}\|_0 + Ch^\sigma\left[\|\mathbf{u}-\mathbf{\Pi}_{\mathrm{N}}\mathbf{u}\|_{\mathrm{curl}} + \|\mathbf{u}-\mathbf{u}_h\|_{DG}\right], \tag{6.2}$$

with $C > 0$ independent of the mesh size, and σ denoting the parameter in (3.2). Inserting (6.2) into (6.1) then proves Theorem 3.5.

In order to prove (6.2), we proceed in several steps.

Step 1. Preliminaries: we start by invoking the Helmholtz decomposition in (4.3) and write

$$\mathbf{\Pi}_{\mathrm{N}}\mathbf{u} - \mathbf{u}_h^c =: \mathbf{w}_0^c \oplus \nabla r, \tag{6.3}$$

with $\mathbf{w}_0^c \in \mathbf{X}_h$ and $r \in S_h$, $\mathbf{X}_h$ and S_h being the spaces in (4.4). By using (6.3) and the orthogonality property of the error $\mathbf{u} - \mathbf{u}_h$ in Proposition 4.10, we have

$$(\mathbf{u} - \mathbf{u}_h, \mathbf{\Pi}_{\mathrm{N}}\mathbf{u} - \mathbf{u}_h^c) = (\mathbf{u} - \mathbf{u}_h, \mathbf{w}_0^c) = (\mathbf{u} - \mathbf{u}_h, \mathbf{w}_0^c - \mathbf{w}) + (\mathbf{u} - \mathbf{u}_h, \mathbf{w}),$$

where we have defined $\mathbf{w} := \mathbf{H}\mathbf{w}_0^c$, the exactly divergence-free approximation of $\mathbf{w}_0^c$ from Lemma 4.4. Therefore,

$$\frac{|(\mathbf{u} - \mathbf{u}_h, \mathbf{\Pi}_{\mathrm{N}}\mathbf{u} - \mathbf{u}_h^c)|}{\|\mathbf{u} - \mathbf{u}_h\|_0} \leq \|\mathbf{w}_0^c - \mathbf{w}\|_0 + \|\mathbf{w}\|_0, \tag{6.4}$$

so that it remains to estimate $\|\mathbf{w}_0^c - \mathbf{w}\|_0$ and $\|\mathbf{w}\|_0$.

Step 2: Estimate of $\|\mathbf{w}_0^c - \mathbf{w}\|_0$*:* we claim that

$$\|\mathbf{w}_0^c - \mathbf{w}\|_0 \leq Ch^\sigma \big[\|\mathbf{u} - \mathbf{\Pi}_{\mathrm{N}}\mathbf{u}\|_{\mathrm{curl}} + \|\mathbf{u} - \mathbf{u}_h\|_{DG}\big], \tag{6.5}$$

with a constant $C > 0$ independent of the mesh size.

To prove (6.5), note that, in view of the definition of $\mathbf{H}$ and (6.3), there holds

$$\nabla \times \mathbf{w} = \nabla \times \mathbf{w}_0^c = \nabla \times (\mathbf{\Pi}_{\mathrm{N}}\mathbf{u} - \mathbf{u}_h^c). \tag{6.6}$$

Thus, the result in Lemma 4.4, the triangle inequality and Proposition 4.7 yield

$$\begin{aligned}
\|\mathbf{w}_0^c - \mathbf{w}\|_0 &\leq Ch^\sigma \|\nabla \times (\mathbf{\Pi}_{\mathrm{N}}\mathbf{u} - \mathbf{u}_h^c)\|_0 \\
&\leq Ch^\sigma \big[\|\nabla \times (\mathbf{\Pi}_{\mathrm{N}}\mathbf{u} - \mathbf{u})\|_0 + \|\nabla_h \times (\mathbf{u} - \mathbf{u}_h)\|_0 + \|\nabla_h \times (\mathbf{u}_h - \mathbf{u}_h^c)\|_0\big] \\
&\leq Ch^\sigma \big[\|\mathbf{u} - \mathbf{\Pi}_{\mathrm{N}}\mathbf{u}\|_{\mathrm{curl}} + \|\mathbf{u} - \mathbf{u}_h\|_{DG}\big].
\end{aligned}$$

This completes the proof of (6.5).

Step 3: Estimate of $\|\mathbf{w}\|_0$*:* we bound $\|\mathbf{w}\|_0$ in (6.4) employing a duality approach and claim that, for a sufficiently small mesh size, there holds

$$\|\mathbf{w}\|_0 \leq C\|\mathbf{u} - \mathbf{\Pi}_{\mathrm{N}}\mathbf{u}\|_0 + Ch^\sigma \big[\|\mathbf{u} - \mathbf{\Pi}_{\mathrm{N}}\mathbf{u}\|_{\mathrm{curl}} + \|\mathbf{u} - \mathbf{u}_h\|_{DG}\big], \tag{6.7}$$

with a constant $C > 0$ independent of the mesh size.

Let $\mathbf{z}$ be the solution of the dual problem (5.4) with right-hand side $\mathbf{w} = \mathbf{H}\mathbf{w}_0^c$. Again, $\mathbf{w} \in H(\mathrm{div}^0; \Omega)$, so that $\mathbf{z}$ has the same smoothness as in the proof of Proposition 5.2 and (5.5) still holds. Moreover, let $\mathbf{z}_h \in \mathbf{V}_h$ solve the discontinuous Galerkin approximation of the dual problem (5.4):

$$\widetilde{a}_h(\mathbf{z}_h, \mathbf{v}) = (\mathbf{w}, \mathbf{v}) \qquad \forall \mathbf{v} \in \mathbf{V}_h. \tag{6.8}$$

For a sufficiently small mesh size, Theorem 3.2 and Corollary 3.4 apply to (6.8) and ensure existence and uniqueness of $\mathbf{z}_h$, as well as the a-priori bound

$$\|\mathbf{z} - \mathbf{z}_h\|_{DG} \leq Ch^\sigma \big[\|\mathbf{z}\|_\sigma + \|\nabla \times \mathbf{z}\|_\sigma\big] \leq Ch^\sigma \|\mathbf{w}\|_0, \tag{6.9}$$

where we have taken into account the stability bound (5.5).

After these preliminary considerations, we multiply equation (5.4) by $\mathbf{w}$ and integrate by parts to obtain

$$\|\mathbf{w}\|_0^2 = a(\mathbf{z},\mathbf{w}) = a(\mathbf{z}-\mathbf{\Pi}^c\mathbf{z},\mathbf{w}) + a(\mathbf{\Pi}^c\mathbf{z},\mathbf{w}), \tag{6.10}$$

with the projection $\mathbf{\Pi}^c$ from (4.10). By the definition of the projection $\mathbf{\Pi}^c$ and since $\nabla\times\mathbf{w} = \nabla\times\mathbf{w}_0^c$, we conclude that

$$\begin{aligned} a(\mathbf{z}-\mathbf{\Pi}^c\mathbf{z},\mathbf{w}) &= -(\mathbf{z}-\mathbf{\Pi}^c\mathbf{z},\mathbf{w}_0^c) - k^2(\mathbf{z}-\mathbf{\Pi}^c\mathbf{z},\mathbf{w}) \\ &= -(\mathbf{z}-\mathbf{\Pi}^c\mathbf{z},\mathbf{w}_0^c-\mathbf{w}) - (1+k^2)(\mathbf{z}-\mathbf{\Pi}^c\mathbf{z},\mathbf{w}). \end{aligned}$$

The approximation result for $\mathbf{\Pi}^c$ in Lemma 4.2 and the bound in (5.5) yield

$$\|\mathbf{z}-\mathbf{\Pi}^c\mathbf{z}\|_0 \le \|\mathbf{z}-\mathbf{\Pi}^c\mathbf{z}\|_{\mathrm{curl}} \le Ch^\sigma\|\mathbf{w}\|_0. \tag{6.11}$$

For later use, we also point out that the stability of $\mathbf{\Pi}^c$ and (5.5) give

$$\|\mathbf{\Pi}^c\mathbf{z}\|_0 \le C\|\mathbf{w}\|_0. \tag{6.12}$$

Hence, the Cauchy-Schwarz inequality and the estimates (6.5) and (6.11) yield

$$\begin{aligned} |a(\mathbf{z}-\mathbf{\Pi}^c\mathbf{z},\mathbf{w})| &\le \|\mathbf{z}-\mathbf{\Pi}^c\mathbf{z}\|_0\|\mathbf{w}-\mathbf{w}_0^c\|_0 + C\|\mathbf{z}-\mathbf{\Pi}^c\mathbf{z}\|_0\|\mathbf{w}\|_0 \\ &\le Ch^{2\sigma}\|\mathbf{w}\|_0\big[\|\mathbf{u}-\mathbf{\Pi}_{\mathrm{N}}\mathbf{u}\|_{\mathrm{curl}} + \|\mathbf{u}-\mathbf{u}_h\|_{DG}\big] + Ch^\sigma\|\mathbf{w}\|_0^2. \end{aligned} \tag{6.13}$$

It remains to bound the term $a(\mathbf{\Pi}^c\mathbf{z},\mathbf{w})$ in (6.10). To this end, in view of (6.6) and (6.3), we first note that

$$\begin{aligned} a(\mathbf{\Pi}^c\mathbf{z},\mathbf{w}) &= (\nabla\times\mathbf{\Pi}^c\mathbf{z},\nabla\times\mathbf{w}) - k^2(\mathbf{\Pi}^c\mathbf{z},\mathbf{w}) \\ &= (\nabla\times\mathbf{\Pi}^c\mathbf{z},\nabla\times(\mathbf{\Pi}_{\mathrm{N}}\mathbf{u}-\mathbf{u}_h^c)) - k^2(\mathbf{\Pi}^c\mathbf{z},\mathbf{w}-\mathbf{w}_0^c) - k^2(\mathbf{\Pi}^c\mathbf{z},\mathbf{w}_0^c) \\ &= (\nabla\times\mathbf{\Pi}^c\mathbf{z},\nabla\times(\mathbf{\Pi}_{\mathrm{N}}\mathbf{u}-\mathbf{u}_h^c)) - k^2(\mathbf{\Pi}^c\mathbf{z},\mathbf{w}-\mathbf{w}_0^c) - k^2(\mathbf{\Pi}^c\mathbf{z},\mathbf{\Pi}_{\mathrm{N}}\mathbf{u}-\mathbf{u}_h^c) \\ &= a(\mathbf{\Pi}^c\mathbf{z},\mathbf{\Pi}_{\mathrm{N}}\mathbf{u}-\mathbf{u}_h^c) - k^2(\mathbf{\Pi}^c\mathbf{z},\mathbf{w}-\mathbf{w}_0^c). \end{aligned}$$

Here, we have used that

$$(\mathbf{\Pi}^c\mathbf{z},\nabla r) = (\mathbf{z},\nabla r) = 0,$$

which follows readily from the definition of $\mathbf{\Pi}^c$ and the fact that $\mathbf{z}$ is divergence-free. From the identity *(i)* in Lemma 4.8, we further have

$$a(\mathbf{\Pi}^c\mathbf{z},\mathbf{\Pi}_{\mathrm{N}}\mathbf{u}-\mathbf{u}_h^c) = a(\mathbf{\Pi}^c\mathbf{z},\mathbf{\Pi}_{\mathrm{N}}\mathbf{u}-\mathbf{u}) + \widetilde{a}_h(\mathbf{\Pi}^c\mathbf{z},\mathbf{u}-\mathbf{u}_h) + \widetilde{a}_h(\mathbf{\Pi}^c\mathbf{z},\mathbf{u}_h-\mathbf{u}_h^c).$$

Using the symmetry of $\widetilde{a}_h(\cdot,\cdot)$, the error equation (4.14), and part *(i)* of Lemma 4.9, we note that $\widetilde{a}_h(\mathbf{\Pi}^c\mathbf{z},\mathbf{u}-\mathbf{u}_h)=0$. Thus, by further decompositions, we can write

$$\begin{aligned} a(\mathbf{\Pi}^c\mathbf{z},\mathbf{w}) =& a(\mathbf{\Pi}^c\mathbf{z}-\mathbf{z},\mathbf{\Pi}_{\mathrm{N}}\mathbf{u}-\mathbf{u}) + a(\mathbf{z},\mathbf{\Pi}_{\mathrm{N}}\mathbf{u}-\mathbf{u}) \\ &+ \widetilde{a}_h(\mathbf{\Pi}^c\mathbf{z}-\mathbf{z},\mathbf{u}_h-\mathbf{u}_h^c) + \widetilde{a}_h(\mathbf{z}-\mathbf{z}_h,\mathbf{u}_h-\mathbf{u}_h^c) \\ &+ \widetilde{a}_h(\mathbf{z}_h,\mathbf{u}_h-\mathbf{u}_h^c) - k^2(\mathbf{\Pi}^c\mathbf{z},\mathbf{w}-\mathbf{w}_0^c), \end{aligned} \tag{6.14}$$

with $\mathbf{z}_h$ denoting the approximation (6.8) of the dual problem (5.4).

Using the dual problem (5.4) and the discrete formulation (6.8), we have

$$a(\mathbf{z},\mathbf{\Pi}_{\mathrm{N}}\mathbf{u}-\mathbf{u}) = (\mathbf{w},\mathbf{\Pi}_{\mathrm{N}}\mathbf{u}-\mathbf{u}), \qquad \widetilde{a}_h(\mathbf{z}_h,\mathbf{u}_h-\mathbf{u}_h^c) = (\mathbf{w},\mathbf{u}_h-\mathbf{u}_h^c).$$

These identities, together with the continuity property *(ii)* in Lemma 4.8 and the Cauchy-Schwarz inequality, give

$$\begin{aligned}|a(\mathbf{\Pi}^c\mathbf{z},\mathbf{w})| \leq & C\|\mathbf{z}-\mathbf{\Pi}^c\mathbf{z}\|_{\mathrm{curl}}\|\mathbf{u}-\mathbf{\Pi}_{\mathrm{N}}\mathbf{u}\|_{\mathrm{curl}} + \|\mathbf{w}\|_0\|\mathbf{u}-\mathbf{\Pi}_{\mathrm{N}}\mathbf{u}\|_0 \\ & + C\|\mathbf{u}_h-\mathbf{u}_h^c\|_{DG}\Big[\|\mathbf{z}-\mathbf{\Pi}^c\mathbf{z}\|_{\mathrm{curl}} + \|\mathbf{z}-\mathbf{z}_h\|_{DG}\Big] \\ & + \|\mathbf{w}\|_0\|\mathbf{u}_h-\mathbf{u}_h^c\|_0 + C\|\mathbf{\Pi}^c\mathbf{z}\|_0\|\mathbf{w}-\mathbf{w}_0^c\|_0.\end{aligned}$$

From Proposition 4.7, we have

$$\|\mathbf{u}_h-\mathbf{u}_h^c\|_{DG} \leq C\|\mathbf{u}-\mathbf{u}_h\|_{DG}, \qquad \|\mathbf{u}_h-\mathbf{u}_h^c\|_0 \leq Ch\|\mathbf{u}-\mathbf{u}_h\|_{DG}.$$

Thus, using (6.11), (6.9), (6.12) and (6.5), we conclude that

$$a(\mathbf{\Pi}^c\mathbf{z},\mathbf{w}) \leq \|\mathbf{w}\|_0\Big[Ch^\sigma\|\mathbf{u}-\mathbf{\Pi}_{\mathrm{N}}\mathbf{u}\|_{\mathrm{curl}} + Ch^\sigma\|\mathbf{u}-\mathbf{u}_h\|_{DG} + \|\mathbf{u}-\mathbf{\Pi}_{\mathrm{N}}\mathbf{u}\|_0\Big]. \quad (6.15)$$

Inserting (6.13) and (6.15) into (6.10) results in

$$\|\mathbf{w}\|_0 \leq \|\mathbf{u}-\mathbf{\Pi}_{\mathrm{N}}\mathbf{u}\|_0 + Ch^\sigma\big[\|\mathbf{u}-\mathbf{\Pi}_{\mathrm{N}}\mathbf{u}\|_{\mathrm{curl}} + \|\mathbf{u}-\mathbf{u}_h\|_{DG}\big] + Ch^\sigma\|\mathbf{w}\|_0. \quad (6.16)$$

Hence, for a sufficiently small mesh size, we obtain the result in (6.7).

Step 4. Conclusion: the proof of the bound (6.2) follows now from (6.4), (6.5) and (6.16).

6.2. Proof of Corollary 3.6. To complete the proof of Corollary 3.6, we note that Theorem 3.5, Theorem 3.2 and the approximation property (4.8) in Lemma 4.1 for $\mathbf{\Pi}_{\mathrm{N}}$ result in

$$\|\mathbf{u}-\mathbf{u}_h\|_0 \leq Ch^{\min\{s,\ell\}+\sigma}\big[\|\mathbf{u}\|_s + \|\nabla\times\mathbf{u}\|_s\big] + Ch^{\min\{s+\sigma,\ell+1\}}\|\mathbf{u}\|_{s+\sigma}.$$

Since $\|\mathbf{u}\|_s \leq \|\mathbf{u}\|_{s+\sigma}$ and $\min\{s+\sigma,\ell+1\} \geq \min\{s,\ell\}+\sigma$, the assertion of Corollary 3.6 follows.

7. Numerical experiments. In this section we present a series of numerical experiments to highlight the practical performance of the DG method introduced and analyzed in this article for the numerical approximation of the indefinite time-harmonic Maxwell equations in (1.1). For simplicity, we restrict ourselves to two-dimensional model problems; additionally, we note that throughout this section we select the interior penalty parameter α in (2.4) as follows:

$$\alpha = 10\,\ell^2.$$

The dependence of α on the polynomial degree ℓ has been chosen in order to guarantee the stability property in Lemma 3.1 independently of ℓ, cf. [15], for example.

7.1. Example 1. In this first example we select $\Omega \subset \mathbb{R}^2$ to be the square domain $(-1,1)^2$. Furthermore, we set $\mathbf{j}=\mathbf{0}$ and select suitable non-homogeneous boundary conditions for $\mathbf{u}$ so that the analytical solution to the two-dimensional analogue of (1.1) is given by the smooth field

$$\mathbf{u}(x,y) = (\sin(ky), \sin(kx))^T.$$

Here, the boundary conditions are enforced in the usual DG manner by adding boundary terms in the formulation (2.2); see [15, 13] for details. We investigate the asymptotic convergence of the DG method on a sequence of successively finer (quasi-uniform)

	$\ell=1$		$\ell=2$		$\ell=3$	
Elements	$\|\mathbf{u}-\mathbf{u}_h\|_{DG}$	r	$\|\mathbf{u}-\mathbf{u}_h\|_{DG}$	r	$\|\mathbf{u}-\mathbf{u}_h\|_{DG}$	r
26	1.853e-1	-	2.009e-2	-	5.044e-4	-
104	9.122e-2	1.02	5.004e-3	2.01	6.471e-5	2.96
416	4.455e-2	1.03	1.250e-3	2.00	8.131e-6	2.99
1664	2.194e-2	1.02	3.123e-4	2.00	1.017e-6	3.00
6656	1.088e-2	1.01	7.808e-5	2.00	1.271e-7	3.00

TABLE 7.1
Example 1. Convergence of $\|\mathbf{u}-\mathbf{u}_h\|_{DG}$ *with* $k=1$.

	$\ell=1$		$\ell=2$		$\ell=3$	
Elements	$\|\mathbf{u}-\mathbf{u}_h\|_{DG}$	r	$\|\mathbf{u}-\mathbf{u}_h\|_{DG}$	r	$\|\mathbf{u}-\mathbf{u}_h\|_{DG}$	r
26	1.113	-	1.265e-1	-	1.242e-2	-
104	5.397e-1	1.04	3.217e-2	1.98	1.582e-3	2.97
416	2.635e-1	1.03	8.078e-3	1.99	1.985e-4	2.99
1664	1.302e-1	1.02	2.022e-3	2.00	2.483e-5	3.00
6656	6.477e-2	1.01	5.055e-4	2.00	3.103e-6	3.00

TABLE 7.2
Example 1. Convergence of $\|\mathbf{u}-\mathbf{u}_h\|_{DG}$ *with* $k=2$.

unstructured triangular meshes for $\ell = 1, 2, 3$ as the wave number k increases. To this end, in Tables 7.1, 7.2, 7.3 and 7.4 we present numerical experiments for $k = 1, 2, 4, 8$, respectively. In each case we show the number of elements in the computational mesh, the corresponding DG-norm of the error and the numerical rate of convergence r. Here, we observe that (asymptotically) $\|\mathbf{u}-\mathbf{u}_h\|_{DG}$ converges to zero at the optimal rate $\mathcal{O}(h^\ell)$, for each fixed ℓ and each k, as h tends to zero, as predicted by Theorem 3.2. In particular, we make two key observations: firstly, we note that for a given fixed mesh and fixed polynomial degree, an increase in the wave number k leads to an increase in the DG-norm of the error in the approximation to $\mathbf{u}$. In particular, as pointed out in [1], where curl-conforming finite element methods were employed for the numerical approximation of (1.1), the pre-asymptotic region increases as k increases. This is particularly evident when $k = 8$, cf. Table 7.4. Secondly, we observe that the DG-norm of the error decreases when either the mesh is refined, or the polynomial degree is increased as we would expect for this smooth problem.

Finally, in Figure 7.1 we present a comparison of the $L^2(\Omega)^2$-norm of the error in the approximation to $\mathbf{u}$, with the square root of the number of degrees of freedom in the finite element space $\mathbf{V}_h$. Here, we observe that (asymptotically) $\|\mathbf{u}-\mathbf{u}_h\|_0$ converges to zero at the rate $\mathcal{O}(h^{\ell+1})$, for each fixed ℓ and each k, as h tends to zero. This is in full agreement with the optimal rate predicted by Corollary 3.6 and Remark 3.7.

7.2. Example 2. In this second example, we investigate the performance of the DG method (2.2) for a problem with a non-smooth solution. To this end, let Ω be the L-shaped domain $(-1,1)^2 \setminus [0,1) \times (-1,0]$ and select $\mathbf{j}$ (and suitable non-homogeneous boundary conditions for $\mathbf{u}$) so that the analytical solution $\mathbf{u}$ to the two-dimensional analogue of (1.1) is given, in terms of the polar coordinates (r, ϑ), by

$$\mathbf{u}(x,y) = \nabla S(r,\vartheta), \quad \text{where} \quad S(r,\vartheta) = J_\alpha(kr)\sin(\alpha\vartheta), \tag{7.1}$$

	$\ell = 1$		$\ell = 2$		$\ell = 3$	
Elements	$\|\mathbf{u}-\mathbf{u}_h\|_{DG}$	r	$\|\mathbf{u}-\mathbf{u}_h\|_{DG}$	r	$\|\mathbf{u}-\mathbf{u}_h\|_{DG}$	r
26	3.868	-	1.275	-	1.429e-1	-
104	2.016	0.94	2.971e-1	2.10	2.289e-2	2.64
416	9.871e-1	1.03	7.401e-2	2.01	2.952e-3	2.96
1664	4.865e-1	1.02	1.849e-2	2.00	3.715e-4	2.99
6656	2.415e-1	1.01	4.623e-3	2.00	4.650e-5	3.00

TABLE 7.3
Example 1. Convergence of $\|\mathbf{u}-\mathbf{u}_h\|_{DG}$ *with* $k = 4$.

	$\ell = 1$		$\ell = 2$		$\ell = 3$	
Elements	$\|\mathbf{u}-\mathbf{u}_h\|_{DG}$	r	$\|\mathbf{u}-\mathbf{u}_h\|_{DG}$	r	$\|\mathbf{u}-\mathbf{u}_h\|_{DG}$	r
26	30.73	-	9.018	-	2.451	-
104	9.434	1.70	2.118	2.09	4.051e-1	2.60
416	4.777	0.98	5.396e-1	1.97	5.245e-2	2.95
1664	2.196	1.12	1.363e-1	1.98	6.625e-3	2.99
6656	1.071	1.04	3.420e-2	1.99	8.301e-4	3.00

TABLE 7.4
Example 1. Convergence of $\|\mathbf{u}-\mathbf{u}_h\|_{DG}$ *with* $k = 8$.

where J_α denotes the Bessel function of the first kind and α is a real number. We set $\alpha = 2n/3$, where n is a positive integer; the analytical solution given by (7.1) then contains a singularity at the re-entrant corner located at the origin of Ω. In particular, we note that $\mathbf{u}$ lies in the Sobolev space $H^{2n/3-\varepsilon}(\Omega)^2$, $\varepsilon > 0$. This example represents a slight modification of the numerical experiment presented in [1].

In this example we again consider the convergence of the DG method (2.2) on a sequence of successively finer (quasi-uniform) unstructured triangular meshes for $\ell = 1, 2, 3$ as the wave number k increases. We first consider the case of the strongest singularity when $n = 1$; to this end, in Tables 7.5, 7.6, 7.7 and 7.8 we present numerical experiments for $k = 1, 2, 4, 6$, respectively. Here, we observe that (asymptotically) $\|\mathbf{u}-\mathbf{u}_h\|_{DG}$ converges to zero at the optimal rate $\mathcal{O}(h^{\min\{2/3-\varepsilon,\ell\}})$, for each fixed ℓ and each k, as h tends to zero, as predicted by Theorem 3.2. As in the previous example, we see that the DG-norm of the error in the approximation to $\mathbf{u}$ increases as the wave number k increases for a fixed mesh size and polynomial degree; and again, that the pre-asymptotic region increases as k increases. Moreover, even for this non-smooth example, for a fixed mesh and wave number, an increase in the polynomial degree leads to a decrease in $\|\mathbf{u}-\mathbf{u}_h\|_{DG}$; this is also the case, when the DG-norm of the error is compared with the total number of degrees of freedom employed in the underlying finite element space, for each fixed k; for brevity these results have been omitted.

Analogous behavior is also observed when $n = 2$ and $n = 4$; for brevity, in Tables 7.9 and 7.10, we present results for $n = 2$ and $n = 4$, respectively, only for the case when $k = 1$. As before larger wave numbers lead to an increase in the magnitude of the error as well as an increase in the pre-asymptotic region. Here, we again observe that (asymptotically) $\|\mathbf{u}-\mathbf{u}_h\|_{DG}$ converges to zero at the optimal rate $\mathcal{O}(h^{\min\{2n/3-\varepsilon,\ell\}})$, for each fixed ℓ, as h tends to zero, as predicted by Theorem 3.2. One exception occurs when linear elements are employed; indeed, in both cases, we

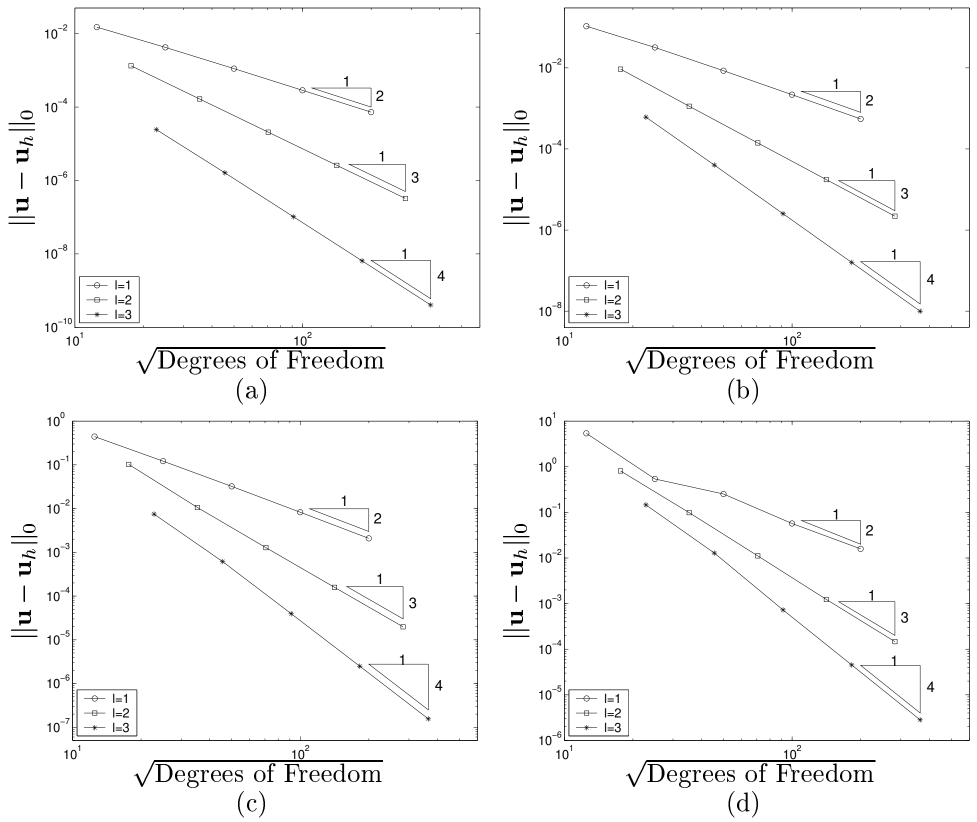

FIG. 7.1. *Example 1. Convergence of* $\|\mathbf{u} - \mathbf{u}_h\|_0$ *for: (a)* $k = 1$*; (b)* $k = 2$*; (c)* $k = 4$*; (d)* $k = 8$.

see that when $\ell = 1$, a slightly superior rate of convergence is attained in practice.

Finally, we end this section by considering the rate of convergence of the error in the approximation to $\mathbf{u}$ measured in terms of the $L^2(\Omega)^2$-norm. To this end, in Figure 7.2 we plot the $L^2(\Omega)^2$-norm of the error in the approximation to $\mathbf{u}$, with the square root of the number of degrees of freedom in the finite element space $\mathbf{V}_h$, for $n = 1, 2, 4$, in the case when $k = 1$. Here, we observe that (asymptotically) $\|\mathbf{u} - \mathbf{u}_h\|_0$ converges to zero at the rate $\mathcal{O}(h^{\min\{2n/3, \ell+1\}})$, for each fixed ℓ, as h tends to zero. In the case of the strongest singularity when $n = 1$, the regularity assumptions required in the statement of Corollary 3.6 do not hold. However, this rate is in agreement with Corollary 3.6 when $n = 2$; in this case the embedding parameter (which only depends on Ω) is $\sigma = 2/3$, cf. [14] and $s = 2/3$. For the case when $n = 4$, we have $s = 2$; thereby, while for $\ell = 2, 3$, the order of convergence of the $L^2(\Omega)^2$-norm of the error is in agreement with Corollary 3.6, the theoretically predicted rate of $\mathcal{O}(h^{5/3})$ for $\ell = 1$ is slightly pessimistic in comparison to the full order $\mathcal{O}(h^2)$ that we observe numerically. Analogous results are attained with higher wave numbers; for brevity, these numerics have been omitted.

	$\ell = 1$		$\ell = 2$		$\ell = 3$	
Elements	$\Vert\mathbf{u}-\mathbf{u}_h\Vert_{DG}$	r	$\Vert\mathbf{u}-\mathbf{u}_h\Vert_{DG}$	r	$\Vert\mathbf{u}-\mathbf{u}_h\Vert_{DG}$	r
24	1.052e-1	-	6.185e-2	-	4.239e-2	-
96	6.175e-2	0.77	3.749e-2	0.72	2.612e-2	0.70
384	3.761e-2	0.72	2.324e-2	0.69	1.631e-2	0.68
1536	2.336e-2	0.69	1.455e-2	0.68	1.024e-2	0.67
6144	1.463e-2	0.68	9.140e-3	0.67	6.439e-3	0.67

TABLE 7.5

Example 2. Convergence of $\Vert\mathbf{u}-\mathbf{u}_h\Vert_{DG}$ *with* $n = 1$ *and* $k = 1$.

	$\ell = 1$		$\ell = 2$		$\ell = 3$	
Elements	$\Vert\mathbf{u}-\mathbf{u}_h\Vert_{DG}$	r	$\Vert\mathbf{u}-\mathbf{u}_h\Vert_{DG}$	r	$\Vert\mathbf{u}-\mathbf{u}_h\Vert_{DG}$	r
24	1.556e-1	-	9.423e-2	-	6.613e-2	-
96	9.493e-2	0.71	5.869e-2	0.68	4.118e-2	0.68
384	5.897e-2	0.69	3.671e-2	0.68	2.582e-2	0.67
1536	3.690e-2	0.68	2.305e-2	0.67	1.623e-2	0.67
6144	2.318e-2	0.67	1.450e-2	0.67	1.022e-2	0.67

TABLE 7.6

Example 2. Convergence of $\Vert\mathbf{u}-\mathbf{u}_h\Vert_{DG}$ *with* $n = 1$ *and* $k = 2$.

	$\ell = 1$		$\ell = 2$		$\ell = 3$	
Elements	$\Vert\mathbf{u}-\mathbf{u}_h\Vert_{DG}$	r	$\Vert\mathbf{u}-\mathbf{u}_h\Vert_{DG}$	r	$\Vert\mathbf{u}-\mathbf{u}_h\Vert_{DG}$	r
24	7.467e-1	-	2.511e-1	-	1.579e-1	-
96	2.561e-1	1.54	1.278e-1	0.97	8.058e-2	0.97
384	1.251e-1	1.03	6.815e-2	0.91	4.507e-2	0.84
1536	6.747e-2	0.89	3.921e-2	0.80	2.683e-2	0.75
6144	3.916e-2	0.79	2.369e-2	0.73	1.649e-2	0.70

TABLE 7.7

Example 2. Convergence of $\Vert\mathbf{u}-\mathbf{u}_h\Vert_{DG}$ *with* $n = 1$ *and* $k = 4$.

	$\ell = 1$		$\ell = 2$		$\ell = 3$	
Elements	$\Vert\mathbf{u}-\mathbf{u}_h\Vert_{DG}$	r	$\Vert\mathbf{u}-\mathbf{u}_h\Vert_{DG}$	r	$\Vert\mathbf{u}-\mathbf{u}_h\Vert_{DG}$	r
24	6.351	-	5.228e-1	-	4.033e-1	-
96	5.394e-1	3.56	3.613e-1	0.53	1.426e-1	1.50
384	2.260e-1	1.26	1.139e-1	1.67	6.983e-2	1.03
1536	1.289e-1	0.81	5.844e-2	0.96	3.810e-2	0.87
6144	5.777e-2	1.16	3.295e-2	0.83	2.238e-2	0.77

TABLE 7.8

Example 2. Convergence of $\Vert\mathbf{u}-\mathbf{u}_h\Vert_{DG}$ *with* $n = 1$ *and* $k = 6$.

	$\ell = 1$		$\ell = 2$		$\ell = 3$	
Elements	$\|\mathbf{u} - \mathbf{u}_h\|_{DG}$	r	$\|\mathbf{u} - \mathbf{u}_h\|_{DG}$	r	$\|\mathbf{u} - \mathbf{u}_h\|_{DG}$	r
24	1.676e-2	-	5.049e-3	-	2.512e-3	-
96	6.138e-3	1.45	2.007e-3	1.33	9.982e-4	1.33
384	2.347e-3	1.39	7.975e-4	1.33	3.962e-4	1.33
1536	9.140e-4	1.36	3.166e-4	1.33	1.573e-4	1.33
6144	3.590e-4	1.35	1.257e-4	1.33	6.242e-5	1.33

TABLE 7.9
Example 2. Convergence of $\|\mathbf{u} - \mathbf{u}_h\|_{DG}$ *with* $n = 2$ *and* $k = 1$.

	$\ell = 1$		$\ell = 2$		$\ell = 3$	
Elements	$\|\mathbf{u} - \mathbf{u}_h\|_{DG}$	r	$\|\mathbf{u} - \mathbf{u}_h\|_{DG}$	r	$\|\mathbf{u} - \mathbf{u}_h\|_{DG}$	r
24	4.811e-3	-	3.059e-4	-	3.214e-5	-
96	1.386e-3	1.80	4.556e-5	2.75	5.108e-6	2.65
384	4.195e-4	1.72	7.041e-6	2.69	8.078e-7	2.66
1536	1.338e-4	1.65	1.119e-6	2.65	1.274e-7	2.66
6144	4.448e-5	1.59	1.817e-7	2.62	2.008e-8	2.67

TABLE 7.10
Example 2. Convergence of $\|\mathbf{u} - \mathbf{u}_h\|_{DG}$ *with* $n = 4$ *and* $k = 1$.

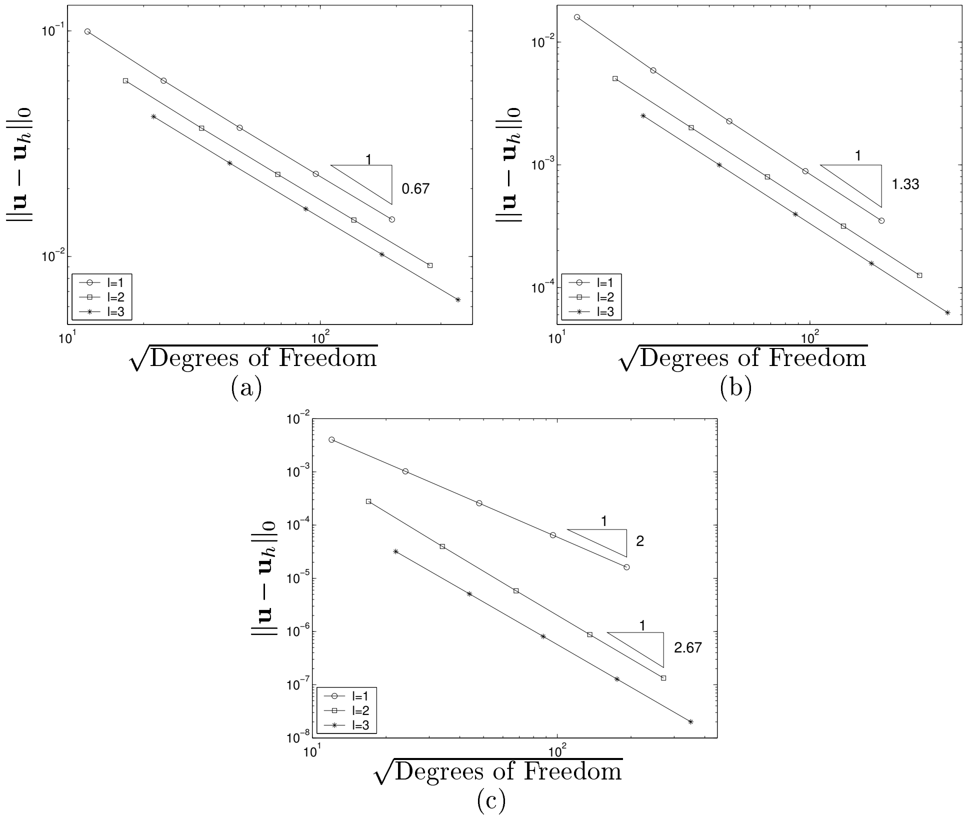

FIG. 7.2. *Example 2. Convergence of* $\|\mathbf{u} - \mathbf{u}_h\|_0$ *when* $k = 1$ *for: (a)* $n = 1$*; (b)* $n = 2$*; (c)* $n = 4$.

8. Conclusions. In this paper, we have presented the *first* a-priori error analysis of the interior penalty discontinuous Galerkin method applied to the *indefinite* time-harmonic Maxwell equations in non-mixed form. In particular, by employing a technique in the spirit of [19, Section 7.2] and [20], combined with a crucial approximation result for discontinuous finite element functions, we have shown that the error in the DG energy norm converges optimally with respect to the mesh size. Under additional regularity assumptions, we have further shown that the error in the L^2-norm converges with the optimal order $\mathcal{O}(h^{\ell+1})$. The extension of our analysis to problems with non-smooth coefficients, by extending more general analysis approaches for conforming methods (such as the ones in [5] or [12]) to the discontinuous Galerkin context, is under investigation.

Appendix A. In this section we prove the approximation result stated in Proposition 4.5; to this end, we proceed in the following steps.

Step 1 (Preliminaries). We begin by introducing the following notation. Recall that each element $K \in \mathcal{T}_h$ is the image of the reference element $\widehat{K}$ under an affine mapping F_K; that is, $K = F_K(\widehat{K})$ for all $K \in \mathcal{T}_h$, where $F_K(\widehat{\mathbf{x}}) = B_K\widehat{\mathbf{x}} + \mathbf{b}_K$ and $B_K \in \mathbb{R}^{3\times 3}$, $\mathbf{b}_K \in \mathbb{R}^3$. Without loss of generality, we assume that $\det B_K > 0$. We define

$$\mathbb{D}^\ell(K) = \{\, \mathbf{q} \,:\, \mathbf{q}\circ F_K = \frac{1}{\det B_K} B_K\widehat{\mathbf{q}},\ \widehat{\mathbf{q}} \in \mathbb{P}^{\ell-1}(\widehat{K})^3 \oplus \widetilde{\mathbb{P}}^{\ell-1}(\widehat{K})\,\widehat{\mathbf{x}}\,\},$$

where $\widetilde{\mathbb{P}}^{\ell-1}(\widehat{K})$ denotes the space of homogeneous polynomials of total degree exactly $\ell-1$ in $\widehat{\mathbf{x}} = (\widehat{x}_1, \widehat{x}_2, \widehat{x}_3)$ on $\widehat{K}$. A polynomial $\mathbf{q} \in \mathbb{D}^\ell(K)$ can be represented as $\mathbf{q}(\mathbf{x}) = \mathbf{r}(\mathbf{x}) + \widetilde{s}(\mathbf{x})\,\mathbf{x}$, with $\mathbf{r} \in \mathbb{P}^{\ell-1}(K)^3$ and $\widetilde{s} \in \widetilde{\mathbb{P}}^{\ell-1}(K)$.

Next, we assign to each face $f \in \mathcal{F}_h$ a unit normal vector $\mathbf{n}_f$. Then there is a unique element $K \in \mathcal{T}_h$ such that $f \subset \partial K$ and f is the image of the corresponding reference face $\widehat{f}$ on $\widehat{K}$ under the elemental mapping F_K, and such that $\mathbf{n}_f = B_K^{-T}\widehat{\mathbf{n}}_{\widehat{f}}/|B_K^{-T}\widehat{\mathbf{n}}_{\widehat{f}}|$, where $\widehat{\mathbf{n}}_{\widehat{f}}$ is the outward unit normal vector to $\widehat{f}$; cf. [19, Equation (5.21)]. We set

$$\mathbb{D}^\ell(f) = \{\, \mathbf{q}|_f \,:\, \mathbf{q}\circ F_K = B_K\widehat{\mathbf{q}},\ \mathbf{q} \in \mathbb{D}^\ell(\widehat{K}),\ \widehat{\mathbf{q}}\cdot\widehat{\mathbf{n}}_{\widehat{f}} = 0\,\}.$$

In local coordinates $\mathbf{x}$ on the face f, a function $\mathbf{q}|_f \in \mathbb{D}^\ell(f)$ is given by $\mathbf{q}|_f(\mathbf{x}) = \mathbf{r}(\mathbf{x}) + \widetilde{s}(\mathbf{x})\,\mathbf{x}$, where $\mathbf{r} \in \mathbb{P}^{\ell-1}(f)^2$ and $\widetilde{s} \in \widetilde{\mathbb{P}}^{\ell-1}(f)$. Notice that $\mathbf{q}|_f$ is tangential to f.

Finally, we assign to each edge e a unit vector $\mathbf{t}_e$ in the direction of e, and denote by $\mathbb{P}^\ell(e)$ the space of polynomials of degree at most ℓ on e.

Step 2 (Moments for Nédélec's elements of the second type). We introduce a basis for $\mathbb{P}^\ell(K)^3$ based on the moments employed in the definition of Nédélec's second family of elements introduced in [21]. Following [19], we use the following moments that are identical on K and $\widehat{K}$, up to sign changes, under the transformation $\mathbf{v}\circ F_K = B_K^{-T}\widehat{\mathbf{v}}$ (this can be easily seen as in [19, Lemma 5.34 and Section 8]).

For an edge e, let $\{q_e^i\}_{i=1}^{N_e}$ denote a basis of $\mathbb{P}^\ell(e)$. Similarly, let $\{\mathbf{q}_f^i\}_{i=1}^{N_f}$ be a basis of $\mathbb{D}^{\ell-1}(f)$ for a face f, and $\{\mathbf{q}_K^i\}_{i=1}^{N_b}$ a basis of $\mathbb{D}^{\ell-2}(K)$ for element K. Fix

$K \in \mathcal{T}_h$ and let $\mathbf{v} \in \mathbb{P}^\ell(K)^3$. We introduce the following moments:

$$M_K^e(\mathbf{v}) = \left\{ \int_e (\mathbf{v} \cdot \mathbf{t}_e) q_e^i \, ds : i = 1, \dots, N_e \right\}, \qquad \text{for any edge } e \text{ of } K,$$
$$M_K^f(\mathbf{v}) = \left\{ \frac{1}{\mathrm{area}(f)} \int_f \mathbf{v} \cdot \mathbf{q}_f^i \, ds : i = 1, \dots, N_f \right\}, \text{ for any face } f \text{ of } K,$$
$$M_K^b(\mathbf{v}) = \left\{ \int_K \mathbf{v} \cdot \mathbf{q}_K^i \, d\mathbf{x} : i = 1, \dots, N_b \right\}.$$

It is well-known that the above moments uniquely define the polynomial $\mathbf{v} \in \mathbb{P}^\ell(K)^3$; see [21, 19]. For a face f of K, the tangential trace $\mathbf{n}_f \times \mathbf{v}$ is uniquely determined by the moments M_K^f and the moments $\{M_K^e\}_{e \in \mathcal{E}(f)}$, where $\mathcal{E}(f)$ is the set of the edges of f; see [21, Section 3.1] or [19, Lemma 8.11]. Hence, any $\mathbf{v} \in \mathbb{P}^\ell(K)^3$ can be written in the form

$$\mathbf{v} = \sum_{e \in \mathcal{E}(K)} \sum_{i=1}^{N_e} v_{K,e}^i \boldsymbol{\varphi}_{K,e}^i + \sum_{f \in \mathcal{F}(K)} \sum_{i=1}^{N_f} v_{K,f}^i \boldsymbol{\varphi}_{K,f}^i + \sum_{i=1}^{N_b} v_{K,b}^i \boldsymbol{\varphi}_{K,b}^i. \tag{A.1}$$

Here, we use $\mathcal{E}(K)$ and $\mathcal{F}(K)$ to denote the sets of edges and faces of K, respectively. The functions $\{\boldsymbol{\varphi}_{K,e}^i\}$, $\{\boldsymbol{\varphi}_{K,f}^i\}$, and $\{\boldsymbol{\varphi}_{K,b}^i\}$ are Lagrange basis functions on $\mathbb{P}^\ell(K)^3$ with respect to the moments given above.

Step 3 (Bound on the elemental $H(\mathrm{curl})$–norm). Let $\mathbf{v} \in \mathbb{P}^\ell(K)^3$ be represented as in (A.1). We prove the following elemental bound on the $H(\mathrm{curl})$–norm in terms of the moments in Step 2: there exists a positive constant C, independent of the mesh size, such that

$$\begin{aligned} & h_K^{-2} \|\mathbf{v}\|_{0,K}^2 + \|\nabla \times \mathbf{v}\|_{0,K}^2 \\ & \leq C h_K^{-1} \left[\sum_{e \in \mathcal{E}(K)} \sum_{i=1}^{N_e} (v_{K,e}^i)^2 + \sum_{f \in \mathcal{F}(K)} \sum_{i=1}^{N_f} (v_{K,f}^i)^2 + \sum_{i=1}^{N_b} (v_{K,b}^i)^2 \right]. \end{aligned} \tag{A.2}$$

On the reference element, this follows from the representation (A.1) and the Cauchy-Schwarz inequality. On a general element K, we note that since the transformation $\mathbf{v} \circ F_K = B_K^{-T} \widehat{\mathbf{v}}$ preserves the moments in Step 2, and that

$$\|\mathbf{v}\|_{0,K}^2 \leq C h_K \|\widehat{\mathbf{v}}\|_{0,\widehat{K}}^2, \qquad \|\nabla \times \mathbf{v}\|_{0,K}^2 \leq C h_K^{-1} \|\widehat{\nabla} \times \widehat{\mathbf{v}}\|_{0,\widehat{K}}^2,$$

with a constant independent of the mesh size (see, e.g., [2, Lemma 5.2]), the bound in (A.2) is obtained.

Step 4 (Bound on the tangential jumps). Given an interior face f, shared by two elements K_1 and K_2, we write $\mathcal{E}(f)$ to denote the set of edges of f. Given $\mathbf{v}_1 \in \mathbb{P}^\ell(K_1)^3$ and $\mathbf{v}_2 \in \mathbb{P}^\ell(K_2)^3$, we prove that, using the representation in (A.1), there exist positive constants C_1 and C_2, independent of the mesh size, such that

$$\int_f |\mathbf{n}_f \times (\mathbf{v}_1 - \mathbf{v}_2)|^2 ds \leq C_1 \left[\sum_{i=1}^{N_f} (v_{K_1,f}^i - v_{K_2,f}^i)^2 + \sum_{e \in \mathcal{E}(f)} \sum_{i=1}^{N_e} (v_{K_1,e}^i - v_{K_2,e}^i)^2 \right],$$

and

$$\left[\sum_{i=1}^{N_f}(v^i_{K_1,f}-v^i_{K_2,f})^2+\sum_{e\in\mathcal{E}(f)}\sum_{i=1}^{N_e}(v^i_{K_1,e}-v^i_{K_2,e})^2\right] \leq C_2\int_f|\mathbf{n}_f\times(\mathbf{v}_1-\mathbf{v}_2)|^2\,ds. \tag{A.3}$$

To see this, we first consider the case where K_1 and K_2 are of reference size. Since the moments on f and on the edges $e\in\mathcal{E}(f)$ uniquely determine the jump $\mathbf{n}_f\times(\mathbf{v}_1-\mathbf{v}_2)$, the claim follows from the equivalence of norms in finite dimensional spaces. For general elements K_1 and K_2, the claim is obtained from a scaling argument taking into account that the transformation $\mathbf{v}\circ F_K=B_K^{-T}\widehat{\mathbf{v}}$ preserves tangential components and the moments in Step 2, modulo sign changes.

The analogous bound holds on the boundary. Let K be the element containing the boundary face f and $\mathbf{v}\in\mathbb{P}^\ell(K)^3$. Using the representation in (A.1), there exist positive constants C_1 and C_2, independent of the mesh size, such that

$$\int_f|\mathbf{n}_f\times\mathbf{v}|^2\,ds\leq C_1\left[\sum_{i=1}^{N_f}(v^i_{K,f})^2+\sum_{e\in\mathcal{E}(f)}\sum_{i=1}^{N_e}(v^i_{K,e})^2\right],$$

and

$$\left[\sum_{i=1}^{N_f}(v^i_{K,f})^2+\sum_{e\in\mathcal{E}(f)}\sum_{i=1}^{N_e}(v^i_{K,e})^2\right]\leq C_2\int_f|\mathbf{n}_f\times\mathbf{v}|^2\,ds.$$

Step 5 (Approximation property). Let us now prove the result in Proposition 4.5. To this end, it is sufficient to show the following result: for $\mathbf{v}\in\mathbf{V}_h$, we have

$$\inf_{\overline{\mathbf{v}}\in\mathbf{V}_h^c}\|\mathbf{v}-\overline{\mathbf{v}}\|_0^2\leq C\|\mathtt{h}^{\frac12}[\![\mathbf{v}]\!]_T\|^2_{\mathcal{F}_h}, \tag{A.4}$$

$$\inf_{\overline{\mathbf{v}}\in\mathbf{V}_h^c}\left[\|\mathbf{v}-\overline{\mathbf{v}}\|_0^2+\|\nabla\times(\mathbf{v}-\overline{\mathbf{v}})\|_0^2\right]\leq C\|\mathtt{h}^{-\frac12}[\![\mathbf{v}]\!]_T\|^2_{\mathcal{F}_h}, \tag{A.5}$$

with a positive constant C, independent of the mesh size.

To prove the claims above, let $\{v^i_{K,e}\}$, $\{v^i_{K,f}\}$ and $\{v^i_{K,b}\}$ denote the moments of $\mathbf{v}$, according to (A.1). Further, we write $N(e)$ to denote the set of all elements that share the edge e, and by $N(f)$ the set of all elements that share the face f. The cardinality of these sets are denoted by $|N(e)|$ and $|N(f)|$, respectively. Due to the shape-regularity of the meshes $\mathcal{T}_h$, we have that $1\leq|N(e)|\leq N$, uniformly in the mesh size; additionally, $1\leq|N(f)|\leq 2$. Let $\overline{\mathbf{v}}\in\mathbf{V}_h^c$ be the unique function whose edge moments are

$$\overline{v}^i_{K,e}=\begin{cases}\frac{1}{|N(e)|}\sum_{K'\in N(e)}v^i_{K',e} & \text{if } e\in\mathcal{E}_h^{\mathcal{I}},\\ 0 & \text{if } e\in\mathcal{E}_h^{\mathcal{B}},\end{cases}$$

$i=1,\dots,N_e$, whose face moments are

$$\overline{v}^i_{K,f}=\begin{cases}\frac{1}{|N(f)|}\sum_{K'\in N(f)}v^i_{K',f} & \text{if } f\in\mathcal{F}_h^{\mathcal{I}},\\ 0 & \text{if } f\in\mathcal{F}_h^{\mathcal{B}},\end{cases}$$

$i = 1, \ldots, N_f$, and whose remaining moments are

$$\overline{v}^i_{K,b} = v^i_{K,b}, \qquad i = 1, \ldots, N_b.$$

Obviously, the function $\overline{\mathbf{v}}$ defined by the above moments belongs to $\mathbf{V}^c_h$.

From the bound in (A.2) in Step 3, we have

$$\begin{aligned} &h_K^{-2} \|\mathbf{v} - \overline{\mathbf{v}}\|^2_{0,K} + \|\nabla \times (\mathbf{v} - \overline{\mathbf{v}})\|^2_{0,K} \\ &\leq C h_K^{-1} \left[\sum_{e \in \mathcal{E}(K)} \sum_{i=1}^{N_e} (v^i_{K,e} - \overline{v}^i_{K,e})^2 + \sum_{f \in \mathcal{F}(K)} \sum_{i=1}^{N_f} (v^i_{K,f} - \overline{v}^i_{K,f})^2 \right]. \end{aligned}$$

Let e first be an interior edge in $\mathcal{E}(K)$ and denote by $\mathcal{F}(e)$ the faces sharing the edge e. For $f \in \mathcal{F}(e)$, we denote by K_f and K'_f the elements that share f. Employing the definition of $\overline{u}^i_{K,e}$, the Cauchy-Schwarz inequality, bound (A.3) from Step 4, and the shape-regularity assumption gives

$$\begin{aligned} \sum_{i=1}^{N_e} (v^i_{K,e} - \overline{v}^i_{K,e})^2 &\leq C \sum_{K' \in N(e)} \sum_{i=1}^{N_e} (v^i_{K,e} - v^i_{K',e})^2 \\ &\leq C \sum_{f \in \mathcal{F}(e)} \sum_{i=1}^{N_e} (v^i_{K_f,e} - v^i_{K'_f,e})^2 \\ &\leq C \sum_{f \in \mathcal{F}(e)} \int_f |[\![\mathbf{v}]\!]_T|^2 \, ds. \end{aligned}$$

An analogous result holds for a boundary edge e.

Similarly, for an interior face $f \in \mathcal{F}(K)$, we have

$$\sum_{i=1}^{N_f} (v^i_{K,f} - \overline{v}^i_{K,f})^2 \leq C \sum_{K' \in N(f)} \sum_{i=1}^{N_f} (v^i_{K,f} - v^i_{K',f})^2 \leq C \int_f |[\![\mathbf{v}]\!]_T|^2 \, ds,$$

where we have again used the bound (A.3) from Step 4. An analogous results holds for boundary faces.

Combining the above estimates yields

$$\begin{aligned} &h_K^{-2} \|\mathbf{v} - \overline{\mathbf{v}}\|^2_{0,K} + \|\nabla \times (\mathbf{v} - \overline{\mathbf{v}})\|^2_{0,K} \\ &\leq C h_K^{-1} \left[\sum_{e \in \mathcal{E}(K)} \sum_{f \in \mathcal{F}(e)} \int_f |[\![\mathbf{v}]\!]_T|^2 \, ds + \sum_{f \in \mathcal{F}(K)} \int_f |[\![\mathbf{v}]\!]_T|^2 \, ds \right]. \end{aligned}$$

Summing over all elements, taking into account the shape-regularity of the mesh, we deduce (A.4) and (A.5).

REFERENCES

[1] M. Ainsworth and J. Coyle. Hierarchic *hp*-edge element families for Maxwell's equations on hybrid quadrilateral/triangular meshes. *Comput. Methods Appl. Mech. Engrg.*, 190:6709–6733, 2001.

[2] A. Alonso and A. Valli. An optimal domain decomposition preconditioner for low-frequency time-harmonic Maxwell equations. *Math. Comp.*, 68:607–631, 1999.

[3] C. Amrouche, C. Bernardi, M. Dauge, and V. Girault. Vector potentials in three-dimensional non-smooth domains. *Math. Models Appl. Sci.*, 21:823–864, 1998.

[4] D.N. Arnold, F. Brezzi, B. Cockburn, and L.D. Marini. Unified analysis of discontinuous Galerkin methods for elliptic problems. *SIAM J. Numer. Anal.*, 39:1749–1779, 2001.

[5] D. Boffi and L. Gastaldi. Edge finite elements for the approximation of Maxwell resolvent operator. *Modél. Math. Anal. Numér.*, 36:293–305, 2002.

[6] F. Brezzi, J. Rappaz, and P.A. Raviart. Finite dimensional approximation of nonlinear problems. Part I: Branches of nonsingular solutions. *Numer. Math.*, 36:1–25, 1980.

[7] A. Buffa. Remarks on the discretization of some non-coercive operator with applications to Maxwell equations with jumping coefficients. Technical report, IMATI-CNR, Pavia, 2003.

[8] A. Buffa, R. Hiptmair, T. von Petersdorff, and C. Schwab. Boundary element methods for Maxwell transmission problems in Lipschitz domains. *Numer. Math.*, 95:459–485, 2003.

[9] L. Demkowicz and L. Vardapetyan. Modeling of electromagnetic absorption/scattering problems using *hp*–adaptive finite elements. *Comput. Methods Appl. Mech. Engrg.*, 152:103–124, 1998.

[10] P. Fernandes and G. Gilardi. Magnetostatic and electrostatic problems in inhomogeneous anisotropic media with irregular boundary and mixed boundary conditions. *Math. Models Methods Appl. Sci.*, 7:957–991, 1997.

[11] J.S. Hesthaven and T. Warburton. High order nodal discontinuous Galerkin methods for the Maxwell eigenvalue problem. Technical report, 2003.

[12] R. Hiptmair. Finite elements in computational electromagnetism. *Acta Numerica*, pages 237–339, 2003.

[13] P. Houston, I. Perugia, and D. Schötzau. Mixed discontinuous Galerkin approximation of the Maxwell operator. Technical Report 02-16, University of Basel, Department of Mathematics, 2002. To appear in SIAM J. Numer. Anal.

[14] P. Houston, I. Perugia, and D. Schötzau. Energy norm a posteriori error estimation for mixed discontinuous Galerkin approximations of the Maxwell operator. Technical report, University of Leicester, Department of Mathematics, 2003.

[15] P. Houston, I. Perugia, and D. Schötzau. *hp*-DGFEM for Maxwell's equations. In F. Brezzi, A. Buffa, S. Corsaro, and A. Murli, editors, *Numerical Mathematics and Advanced Applications ENUMATH 2001*, pages 785–794. Springer-Verlag, 2003.

[16] P. Houston, I. Perugia, and D. Schötzau. Mixed discontinuous Galerkin approximation of the Maxwell operator: Non-stabilized formulation. Technical report, University of Leicester, Department of Mathematics, 2003.

[17] O.A. Karakashian and F. Pascal. A posteriori error estimation for a discontinuous Galerkin approximation of second order elliptic problems. Technical report, University of Tennessee, Department of Mathematics, 2003. Report can be retrieved from: `http://www.math.utk.edu/~ohannes/papers.html`. To appear in SIAM J. Numer. Anal.

[18] P. Monk. A finite element method for approximating the time-harmonic Maxwell equations. *Numer. Math.*, 63:243–261, 1992.

[19] P. Monk. *Finite element methods for Maxwell's equations.* Oxford University Press, New York, 2003.

[20] P. Monk. A simple proof of convergence for an edge element discretization of Maxwell's equations. In C. Carstensen, S. Funken, W. Hackbusch, R. Hoppe, and P. Monk, editors, *Computational electromagnetics*, volume 28 of *Lect. Notes Comput. Sci. Engrg.*, pages 127–141. Springer–Verlag, 2003.

[21] J.C. Nédélec. A new family of mixed finite elements in $\mathbb{R}^3$. *Numer. Math.*, 50:57–81, 1986.

[22] I. Perugia and D. Schötzau. The *hp*-local discontinuous Galerkin method for low-frequency time-harmonic Maxwell equations. *Math. Comp.*, 72:1179–1214, 2003.

[23] I. Perugia, D. Schötzau, and P. Monk. Stabilized interior penalty methods for the time-harmonic Maxwell equations. *Comput. Methods Appl. Mech. Engrg.*, 191:4675–4697, 2002.

[24] A. Schatz. An observation concerning Ritz-Galerkin methods with indefinite bilinear forms. *Math. Comp.*, 28:959–962, 1974.

[25] L. Vardapetyan and L. Demkowicz. *hp*-adaptive finite elements in electromagnetics. *Comput. Methods Appl. Mech. Engrg.*, 169:331–344, 1999.